a reduction in cortical glial fibrillary acidic protein (GFAP), a typical marker protein for astrocytes (das Neves et al., 1999; Steele-Perkins et al., 2005), as well as a reduction in the number of midline glia (Shu et al., 2003). It was further shown that E18.5 embryos lacking either NFIA or NFIB displayed a reduction in spinal cord GFAP expression (Deneen et al., 2006), and that misexpression of NFIA or NFIB was sufficient to accelerate GFAP expression in astrocytic precursors by several days in vivo and in vitro. These data indicate that NFIA/B promote the terminal differentiation of astrocytes. Furthermore, *gfap* expression is likely to be directly regulated by NFIA/B, as functional NFI-binding sites have been identified in the promoter (Cebolla and Vallejo, 2006). However, the precise relationships between NFIs and other factors, such as the JAK-STAT and Notch signaling pathways and DNA methylation, in the regulation of astrocyte differentiation of NPCs have not been elucidated.

Many studies have provided us with an integrated view of the gliogenic switch, with multiple extrinsic and intrinsic mechanisms acting in concert to induce gliogenesis when an appropriate number of neurons has been generated. Nevertheless, how promoter methylation changes are induced, and why neurons have to be produced first from NPCs during brain development, remain outstanding questions. In this study, we provide an explanation for the sequential differentiation of NPCs into neurons and then astrocytes through the epigenetic modification during embryonic brain development.

RESULTS

Neurons Confer Astrocyte Differentiation Potential on NPCs via Notch Signal Activation

It has been suggested that neuron-secreted CT-1 induces astrocytic differentiation of mouse NPCs at E13.5. However, CT-1 and leukemia inhibitory factor (LIF), which activates the same signaling pathway as CT-1, failed to do so at an earlier stage (E11.5), and did not evoke demethylation of the astrocyte-specific *gfap* gene promoter (Figures 1A and 1D and data not shown). We therefore sought to examine the involvement of cell-to-cell interactions, in addition to that of secreted factors. As a first step, we cocultured E11.5 NPCs with embryonic cortical neurons, and found that they could differentiate into GFAP-positive astrocytes in the presence of LIF (Figures 1B, 1B′, and 1D). Notch signaling is one of the most important mediators of intercellular interaction during CNS development (Louvi and Artavanis-Tsakonas, 2006). Several recent studies have suggested that Notch1 is activated in proliferating NSCs (Tokunaga et al., 2004; Androutsellis-Theotokis et al., 2006; Yoshimatsu et al., 2006), and may play a decisive role in promoting glial development (Grandbarbe et al., 2003). When we performed the same coculture experiment as above, but with a γ-secretase inhibitor (N-[N-(3,5-Difluorophenacetyl-L-Alanyl)]-S-phenylglycine t-butyl ester) to inhibit cleavage of NICD, which is indispensable for Notch signal activation (Androutsellis-Theotokis et al., 2006), astrocytic differentiation was abolished (Figures 1C, 1C′, and 1D). Moreover, ectopic expression of the intracellular-acting Notch signal inhibitor *Dll3* (Ladi et al., 2005) in E11.5 NPCs also resulted in the inhibition of astrocytic differentiation in coculture conditions (see Figure S1 available online). Using the TP1-Venus Notch-activation reporter plasmid (Kohyama et al., 2005), we further confirmed that Notch signaling was indeed activated in NPCs located in close contact with embryonic cortical neurons (Figure S2). These data implicated Notch signaling in the embryonic neuron-induced potentiation of NPCs to differentiate into astrocytes.

Activation of Notch Signal Is Sufficient for Acquisition of Astrocyte Differentiation in NPCs

Next, we sought to determine whether Notch activation is sufficient for astrocytic differentiation of midgestational NPCs. E11.5 NPCs were infected with retroviruses engineered to express either green fluorescent protein (GFP) alone or GFP together with NICD (Takizawa et al., 2003). The following day, LIF was added to the culture, and the cells were incubated for an additional 3 days. In contrast to NPCs infected with control virus, a dramatic induction of GFAP-positive astrocytic differentiation was observed in NICD-expressing NPCs after LIF stimulation (Figures 1F–1G), indicating that the activation of Notch signaling enabled precocious astrocytic differentiation of midgestational NPCs that would otherwise differentiate only into neurons. In the absence of LIF, no GFAP-positive cells were observed in control or NICD-expressing NPCs (data not shown). Thus, although these experiments demonstrated that Notch activation confers astrogliogenic potential on midgestational NPCs, LIF stimulation was still required to induce differentiation of NPCs into GFAP-positive astrocytes.

Since an inverse correlation exists between the potential of NPCs to express *gfap* and the methylation status of the STAT3-binding site within the *gfap* promoter (Fan et al., 2005; Takizawa et al., 2001), we wished to determine whether NICD expression induces demethylation of this site. Four days after virus infection, GFP-positive cells were sorted by fluorescence-activated cell sorting (FACS) and their genomic DNA was subjected to bisulfite sequencing. In freshly prepared E11.5 NPCs, the STAT3 binding site was highly methylated (Figures 1H and 1I), as has been shown previously (Takizawa et al., 2001). The STAT3 site became slightly and spontaneously demethylated in control virus-infected cells during the 4-day culture. In marked contrast, demethylation was dramatically accelerated in NICD-expressing NPCs (Figures 1H and 1I). Another astrocyte-specific gene (*S100β*) promoter was also demethylated by expression of NICD in these cells (Figure S3). These results confirm that the activation of Notch signaling is sufficient to endow E11.5 NPCs with the ability to differentiate into astrocytes by inducing demethylation of astrocytic gene promoters.

Committed Neuronal Precursors and Young Neurons, Pregenerated from NPCs, Express Notch Ligands

It was previously shown that Notch signaling is activated in cells adjacent to MASH1/NEUROGENIN (NGN)-expressing cells in the fetal ventricular zones (VZs) (Tokunaga et al., 2004), and that NGNs induce expression of the Notch ligand, DELTA LIKE 1 (DLL1), in neuronal precursors (Castro et al., 2006). Thus, to obtain direct evidence for an interaction between NGN-expressing cells and NPCs through Notch signaling in vivo, we examined spatiotemporal patterning of Notch activation and expression of its ligand in the mouse embryonic forebrain. We observed that Notch signal-activated cells existed in the cortical VZ at E11.5

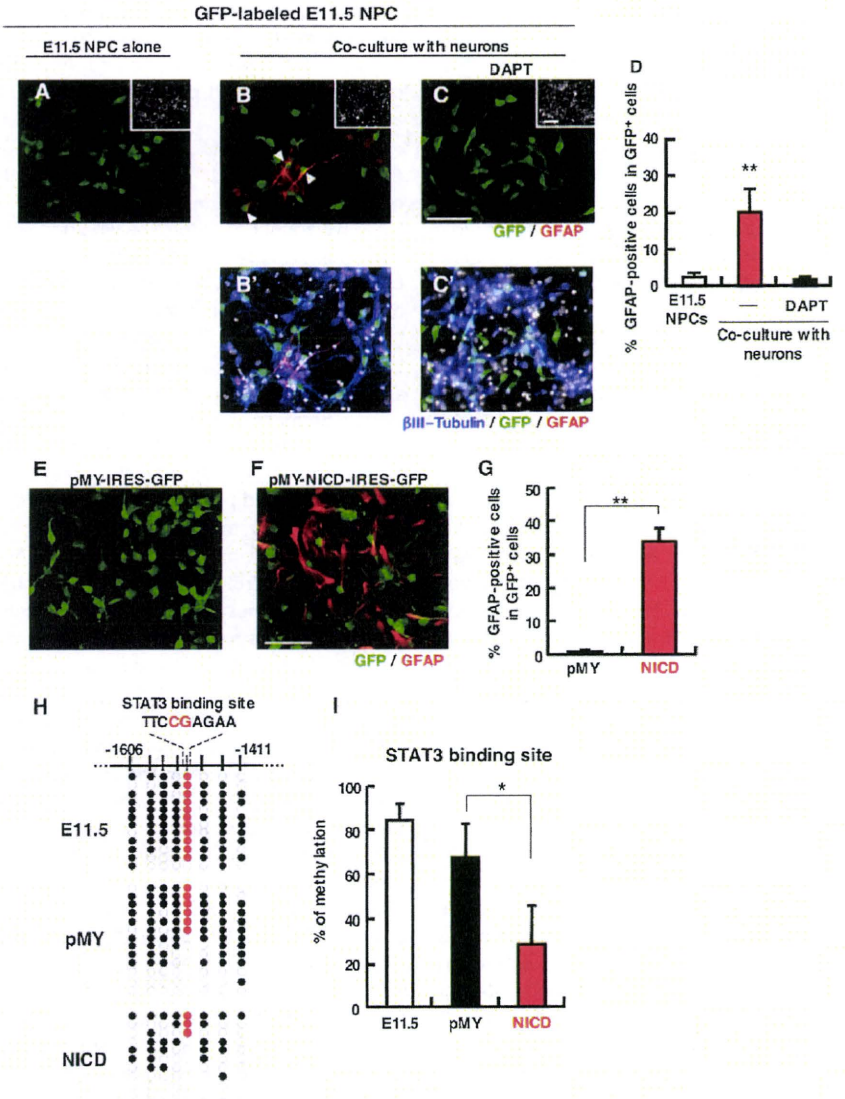

Figure 1. Pregenerated Neurons Potentiate NPCs to Differentiate into Astrocytes via Notch Signal Activation

(A and B) E11.5 NPCs labeled with GFP were cultured alone (A) or with embryonic cortical neurons (B) in the presence of LIF (80 ng/ml) for 4 days.

(C) Coculture as in (B) was performed in the presence of the γ-secretase inhibitor, N-[N-(3,5-Difluorophenacetyl-L-Alanyl)]-S-phenylglycine t-butyl ester (DAPT). After 4 days, the cells in (A)–(C) were stained with antibodies against GFP (green) and GFAP (red). Insets: H33258 nuclear staining of each field. (B′ and C′) β III-tubulin (blue) and H33258 nuclear staining (gray) are superimposed on (B) and (C). Scale bar = 50 μm.

(D) GFAP-positive astrocytes in GFP-positive cells were quantified. Data represent means ± SD (n = 3). Statistical significance was evaluated by one-way ANOVA (**$p < 0.01$).

(E and F) E11.5 NPCs were infected with retroviruses engineered to express GFP alone (E) or GFP together with NICD (F), cultured for 24 hr in the presence of bFGF, and then stimulated with LIF (80 ng/ml) for a further 3 days to induce astrocyte differentiation. The cells in (E) and (F) were stained with antibodies against GFP (green) and GFAP (red). Scale bar = 50 μm.

(G) GFAP-positive astrocytes in GFP control (pMY) and GFP-NICD-expressing cells were quantified. Data are shown as means ± SD. Statistical significance was examined by the Student t test (**$p < 0.01$).

(H) E11.5 NPCs were infected with GFP control (pMY) and GFP-NICD-expressing retroviruses, and were cultured for 4 days with bFGF. After cell sorting based on GFP fluorescence, genomic DNA was extracted from the cells, and the methylation status of the STAT3 binding site and other CpG sites around this sequence in the *gfap* promoter was examined by bisulfite sequencing. "E11.5" indicates the result obtained for freshly prepared NPCs from forebrain at E11.5. Closed and open circles indicate methylated and unmethylated CpG sites, respectively.

(I) Methylation frequency of the CpG site within the STAT3 binding sequence in the *gfap* promoter. Data are shown as means ± SD (n = 3). Statistical significance was examined by the Student t test (*$p < 0.05$).

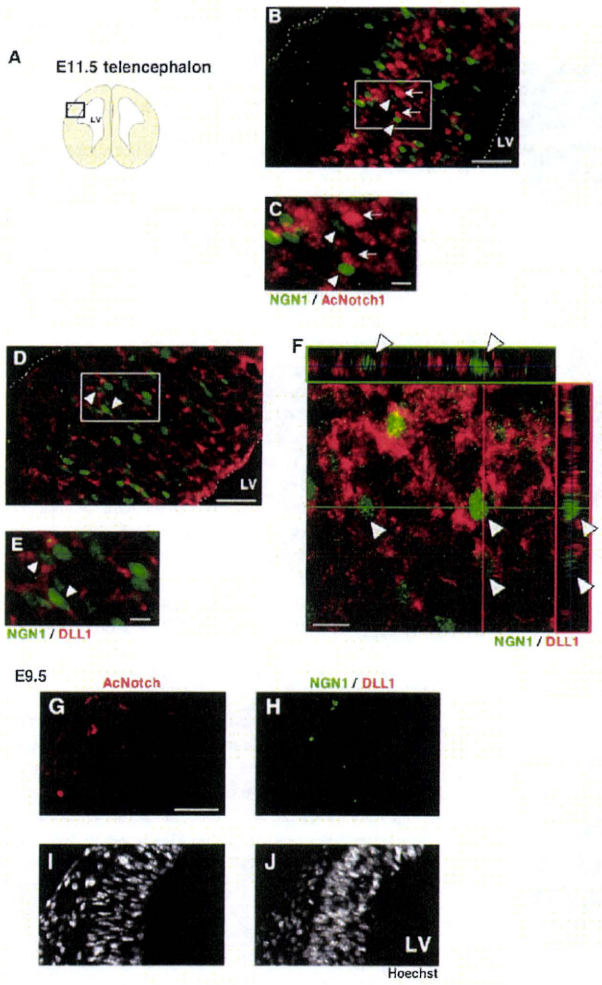

Figure 2. NGN1-Postive Cells Expressing DLL1 and Notch Signal-Activated Cells Are Mutually Exclusive

(A and B) E11.5 forebrain sections (B) from the region illustrated in (A) were immunostained with antibodies against activated Notch (AcNotch, red) and NGN1 (green). Arrows (AcNotch) and arrowheads (NGN1) indicate representatives of each cell type. Notch activation and NGN1 expression were mutually exclusive in these cells. LV, lateral ventricle. Scale bar = 20 μm.

(C) High-magnification view of boxed area in (B). Scale bar = 10 μm.

(D) E11.5 forebrain sections were stained with antibodies against NGN1 (NGN1, green) and DLL1 (DLL1, red). DLL1 was expressed in NGN1-positive differentiating neurons (arrowheads in [D]–[F] mark representatives). Scale bar = 20 μm.

(E) High-magnification view of boxed area in (D). Scale bar = 10 μm.

(F) Coexpression of DLL1 and NGN1 in these cells was confirmed by three-dimensional digital imaging of a brain section immunostained as in (D). Scale bar = 10 μm.

(G and H) E9.5 forebrain sections (12 μm) were stained with antibodies against activated Notch (AcNotch, red) (G), or NGN1 (green) and DLL1 (red) (H). Scale bar = 50 μm.

(I and J) H33258 staining of nuclei of cells in (G) and (H), respectively. No Notch-activated or NGN1-positive cells were observed in VZ at E9.5. LV, lateral ventricle.

(Figures 2A–2C), but not yet at E9.5 (Figures 2G–2J). These results suggest that the timing of Notch signal activation coincides with the onset of demethylation of the *gfap* promoter STAT3 binding site in vivo. Notably, most of the Notch-activated NPCs appeared to be located adjacent to NGN1-expressing cells, and Notch activation and NGN1 expression were mutually exclusive in these cells (Figures 2A–2C). Since NGN1 is a proneural gene product, the expression of which is downregulated when neurons become mature (Schuurmans et al., 2004), we reasoned that cells expressing NGN1 at this stage are either committed neuronal precursors or neurons at very early stages of maturation (Kawaguchi et al., 2008). Furthermore, DLL1 and another Notch ligand, JAGGED1 (JAG1) (Tokunaga et al., 2004; Xue et al., 1999), were expressed in NGN1-expressing cells (Figures 2D–2F; Figures S4A–S4C), consistent with previous reports that *Dll1* is expressed in migrating committed neuronal daughters (intermediate progenitor and young neurons) (Henrique et al., 1995; Castro et al., 2006; Campos et al., 2001; Yoon et al., 2008; Kawaguchi et al., 2008). In agreement with these observations, we found that a significant number of NGN1-positive cells were also positive for T-box brain gene 2, a marker of intermediate progenitor cells (Figures S5A–S5C). On the other hand, Notch-activated NPCs appeared to be radial glial cells, as judged by their morphology through immunostaining with an anti-Nestin antibody (Figures S5D–S5L). Collectively, these data indicate that committed neuronal precursors and young neurons, pregenerated from NPCs, act as a trigger for activation of Notch signaling in adjacent residual NPCs at midgestation.

It should be noted that, although Notch signaling is activated in NPCs at E11.5 in vivo, these NPCs seemed not yet to have the potential to differentiate into GFAP-positive astrocytes when cultured in vitro (Figures 1A, 1C–1E, and 1G). This may be because Notch signal activation had not been underway for long enough to induce the demethylation of astrocytic gene promoters before the NPCs were transferred to in vitro culture, at which point the cell density became sparse compared with that in the brain, leading to insufficient Notch signal activation for the demethylation under these in vitro conditions.

Notch Activation Is Necessary for Astrocyte Differentiation

We next asked whether the Notch downstream molecule, CSL, is involved in Notch-induced demethylation of astrocytic gene promoters in NPCs. To address this, we used CSL-deficient mouse embryonic stem cells (mESCs) (Schroeder et al., 2003), since CSL-deficient embryos die at around E9.5 before neurogenesis in the telencephalon. As has been previously shown, mESC-derived NPCs recapitulate the sequential onset of neuronal and glial differentiation observed in vivo in these cultures (Shimozaki et al., 2005). As expected, at early times in suspension culture, mESC NPCs primarily differentiated into neurons under differentiation-culture conditions, even in the presence of LIF for 4 days (Figure 3A). After 2 weeks in suspension, wild-type (WT) mESC NPCs differentiated into GFAP-positive cells in response to LIF (Figure 3A). In CSL-deficient mESC NPCs, however, no astrocytic differentiation induced by LIF was observed, even after 2 weeks in suspension (Figure 3A). Consistent with these results, the hypermethylated status of

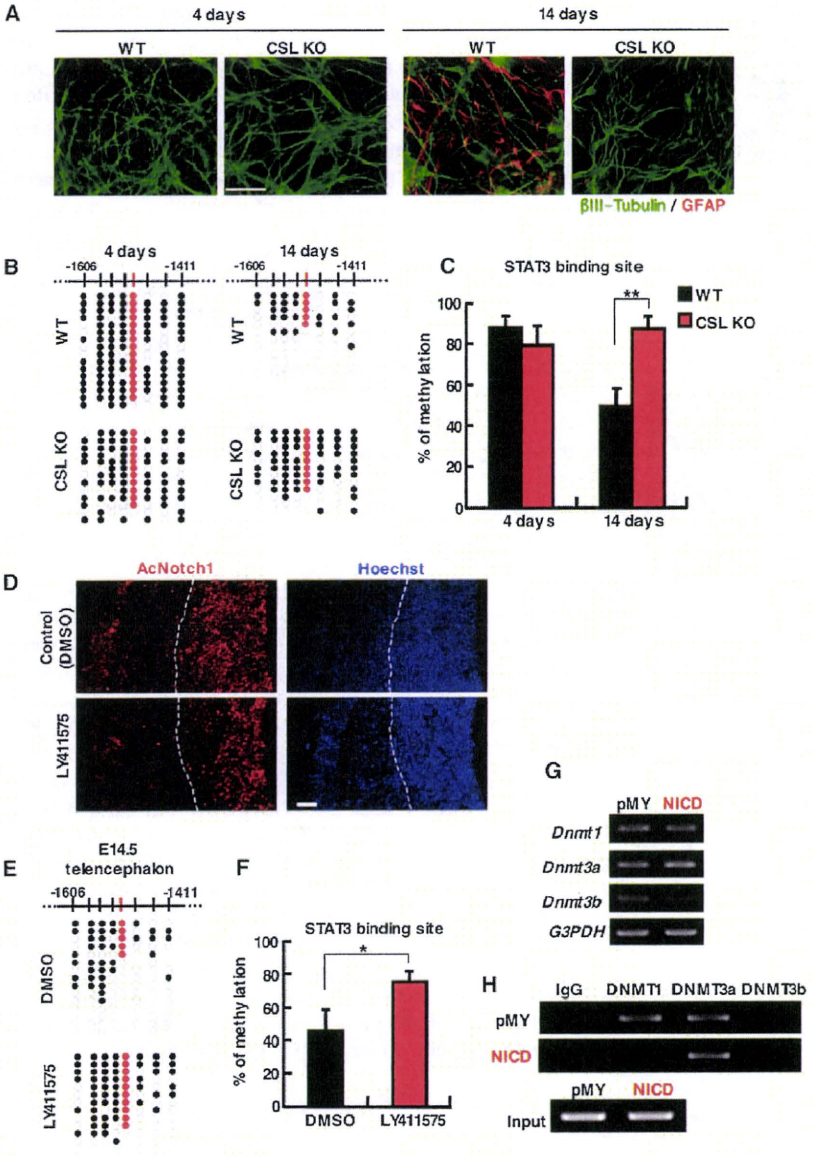

Figure 3. Requirement of CSL for Astrocytic Differentiation and Demethylation of *Gfap* Promoter of NPCs

(A) WT or CSL-deficient (CSL KO) mESCs were cultured in serum-free medium without LIF (neural spheroid, mESC-NPC culture) on poly-HEMA-coated dishes to make suspended aggregates. After 4 or 14 days, the aggregates were dissociated, seeded onto ornithine/fibronectin-coated dishes (monolayer culture) with LIF (80 ng/ml), and incubated for 4 days. Cells were stained with antibodies against a neuronal marker, β-III Tubulin (Tuj1, green), and GFAP (red). LIF-induced GFAP-positive astrocyte differentiation was observed in WT, but not in CSL-deficient mESCs, even after 14 days in suspension. Scale bar = 50 μm.

(B) Bisulfite sequencing results for the CpG site within the STAT3 recognition sequence (red) and other CpG sites around this sequence of the *gfap* promoter in WT and CSL-deficient mESC NPCs cultured as in (A). Each cell type was collected after 4 days in monolayer culture to extract genomic DNA. Closed and open circles indicate methylated and unmethylated CpG sites, respectively.

(C) Methylation frequency of the CpG site within the STAT3 binding sequence in the *gfap* promoter. Data are shown as means ± SD (n = 3). Statistical significance was examined by the Student t test (*$p < 0.05$).

(D) E14.5 forebrain sections of dimethyl sulfoxide (DMSO)- (upper panels) or LY411575 (lower panels)-treated embryonic mice were stained with antibodies against activated Notch (AcNotch in left panels, red). Hoechst staining indicates nuclei (right panels, blue). The white dotted line marks the boundary between the intermediate zone and VZ/SVZ in telencephalon. Scale bar = 50 μm.

(E) Bisulfite sequencing results for the CpG site within the STAT3 recognition sequence (red) and other CpG sites around this sequence of the *gfap* promoter in telencephalon of DMSO- or LY411575-treated embryos.

(F) Methylation frequency of the CpG site within the STAT3 binding sequence in the *gfap* promoter. Data are shown as means ± SD (n = 3). Statistical significance was examined by the Student t test (*$p < 0.05$).

(G) E11.5 NPCs were infected with GFP- or GFP-NICD-expressing virus and cultured for 4 days. After sorting of virus-infected cells based on GFP fluorescence, the expression level of each *Dnmt* gene was examined by RT-PCR.

(H) ChIP assay with specific antibodies for respective DNMTs from GFP- and GFP-NICD-expressing retrovirus-infected NPCs, cultured as in Figure 1G. Dissociation of DNMT1 from the *gfap* promoter was observed in response to NICD expression.

the *gfap* promoter STAT3 site was maintained in CSL-deficient mESC NPCs, compared with WT mESC NPCs (Figures 3B and 3C). Recently, it has been reported that CSL-deficient ESCs are defective in neural precursor generation (Lowell et al., 2006). However, we observed that NPCs can arise from CSL-deficient mESCs in our culture conditions, which are based on methods described previously (Shimozaki et al., 2005), as judged by Nestin or βIII-tubulin staining (Figure 3A and data not shown).

To determine whether the activation of Notch signaling is necessary for demethylation of the astrocyte-specific gene promoter in vivo, we administered the γ-secretase inhibitor, LY411575, to pregnant mice from 10.5 to 13.5 days postcoitum (dpc) and examined the activation of Notch signaling, by immunohistochemistry and by monitoring the methylation status of the *gfap* promoter in E14.5 embryonic telencephalon. As expected, the number of Notch signal-activated cells in the VZ of LY411575-treated embryos was significantly lower than that in control mice (Figure 3D). Moreover, many βIII-tubulin-positive neurons were observed in the VZ of LY411575-treated embryos compared with control mice, suggesting that the disruption of Notch signaling in NPCs leads to an overproduction of neurons

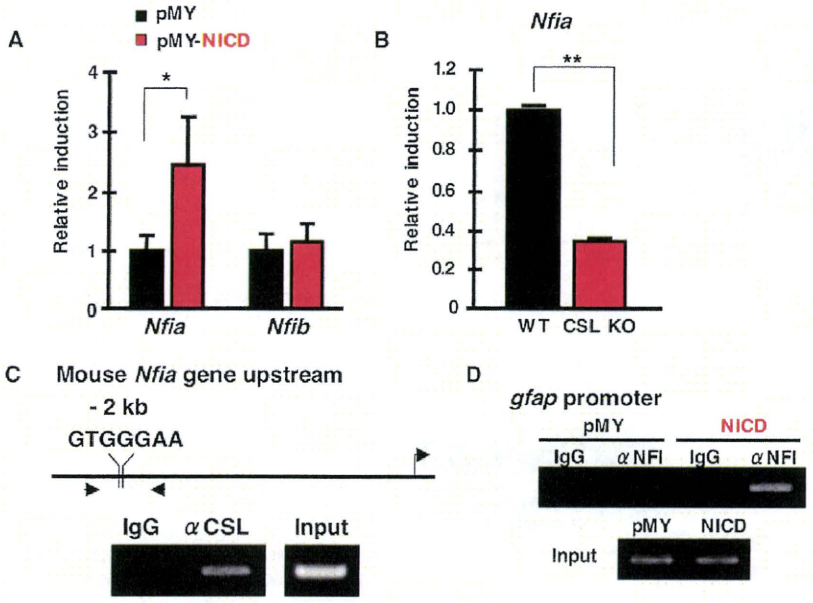

Figure 4. NFI Is a Downstream Molecule of Notch Signaling in NPCs

(A) E11.5 NPCs were infected with GFP- (pMY, closed bars) or GFP-NICD-expressing virus (NICD, red bars) and cultured for 4 days. After sorting of virus-infected cells based on GFP fluorescence, the expression level of *Nfia* and *Nfib* mRNAs was examined by real-time RT-PCR. Data are shown as means ± SD (n = 3). Statistical significance was examined by the Student t test (*$p < 0.05$).

(B) Expression level of *Nfia* mRNA in NPCs derived from ES cells cultured as in (A) (14 days) was examined by real-time RT-PCR. Data are shown as means ± SD (N = 3). Statistical significance was examined by the Student t test (**$p < 0.01$).

(C) ChIP assay of E11.5 NPCs with an antibody against CSL. Binding of CSL to a region containing a CSL cognate sequence located ~2 kb upstream of the *Nfia* transcriptional start site (arrow at right) was detected in E11.5 NPCs.

(D) ChIP assay with an anti-NFI antibody from GFP- and GFP-NICD-expressing retrovirus-infected NPCs cultured as in Figure 1G. Binding of NFI to the *gfap* promoter was observed in response to NICD expression.

(Figure S6A). Consistent with this reduction of Notch signal activation, *gfap* promoter methylation was much higher in the treated embryos than in the controls (Figures 3E and 3F). Furthermore, when we purified NPCs from E14.5 embryos of mice expressing an enhanced GFP (EGFP)transgene under the NPC marker *Sox2* gene promoter (D'Amour and Gage, 2003) by FACS sorting, we observed that the *gfap* promoter in cells from LY411575-treated embryos was hypermethylated compared with its status in control mice (Figures S6B and S6C). We conclude from these experiments that the activation of Notch signaling is prerequisite for demethylation of the astrocyte-specific *gfap* promoter both in vitro and in vivo.

Notch Activation Impairs the Association of Maintenance Methyltransferase with the *gfap* Promoter in NPCs

To establish which DNA methyltransferases (DNMTs) participate in NICD-induced demethylation of the *gfap* promoter, we next examined the expression levels of one maintenance (*Dnmt1*) and two de novo (*Dnmt3a* and *Dnmt3b*) methyltransferase genes by RT-PCR in control and NICD-expressing E11.5 NPCs. Surprisingly, we found no significant differences in *Dnmt* expression between the two cell populations, although *Dnmt3b* expression decreased slightly in NICD-expressing NPCs (Figure 3G). On the other hand, chromatin immunoprecipitation (ChIP) assays with specific antibodies against the three DNMTs revealed that DNMT1 and DNMT3a associated with the *gfap* promoter in the control NPCs (Figure 3H). DNMT1 dissociated from the promoter when Notch signaling was activated (Figure 3H), however, implying that its dissociation may be in part responsible for the Notch-induced demethylation. Moreover, NICD-induced demethylation of the *gfap* promoter was not observed in the absence of basic fibroblast growth factor (bFGF), which is essential for proliferation of NPCs. The proliferation rates of control and NICD-expressing virus-infected cells were similar, as judged by bromodeoxyuridine uptake in the presence of bFGF, ruling out the possibility that selective proliferation of NICD-expressing NPCs occurred (data not shown). Notch-induced demethylation of the astrocytic gene promoter is therefore apparently attributable to passive demethylation: maintenance methylation of genomic DNA, following DNA replication and cell division, fails due to DNMT1 dissociation from the promoter.

NFI Acts as a Critical Molecule Downstream of the Notch Signaling Pathway to Potentiate Astrocytic Differentiation of Midgestational NPCs

A recognition sequence for NFI (Gronostajski, 2000), which is known to play an important role in migration and differentiation of astrocyte precursors (Deneen et al., 2006), has been identified in the *gfap* promoter, and is conserved among human, rat, and mouse (Krohn et al., 1999). We thus next examined whether *Nfi*-family gene expression is upregulated by Notch activation, and found that the expression of *Nfia* indeed increased (Figure 4A). Moreover, its expression was reduced markedly in NPCs from CSL-deficient mESCs compared with that in NPCs from WT mESCs (Figure 4B). We also identified a consensus CSL-binding sequence ~2 kb upstream of the *Nfia* transcription start site, and binding of CSL to this region in NPCs was confirmed (Figure 4C). Furthermore, Notch activation led to binding of NFI to the *gfap* promoter (Figure 4D). To determine whether NFIA expression depends on the activation of Notch signaling, we examined NFIA expression by immunohistochemistry in the telencephalon of LY411575-treated embryos. The area of the VZ occupied by NFIA-positive cells was significantly reduced in LY411575-treated embryos (Figure S7), supporting the scenario that NFIA expression is controlled by the activation of Notch signaling in NPCs.

These results implied that NFI is involved in the Notch-induced potentiation of NPCs to differentiate precociously into astrocytes. To test this notion, E11.5 NPCs were infected with

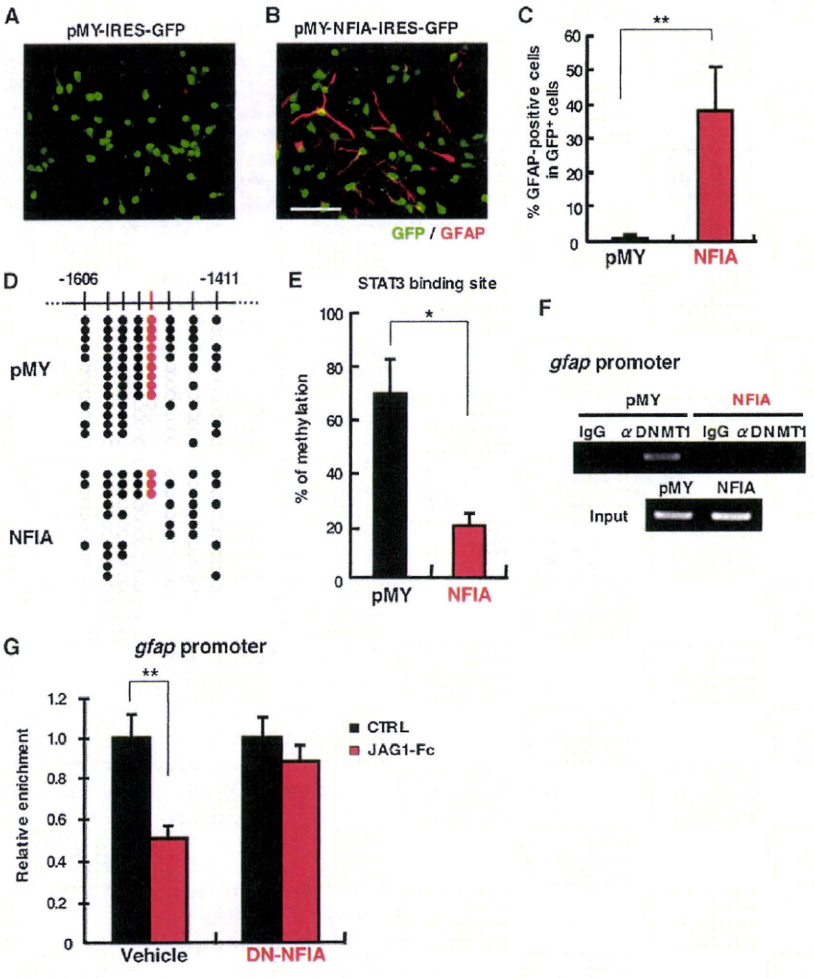

Figure 5. NFI Functions as a Critical Downstream Molecule Mediating Notch Signaling to Potentiate Astrocytic Differentiation of Midgestational NPCs

(A and B) E11.5 NPCs were infected with retroviruses engineered to express GFP alone (A) or GFP together with NFIA (B), cultured for 24 hr in the presence of bFGF, and then stimulated with LIF (80 ng/ml) for a further 3 days to induce astrocytic differentiation. The cells were stained with antibodies against GFP (green) and GFAP (red). Scale bar = 50 μm.

(C) GFAP-positive astrocytes in GFP control (pMY) and GFP-NFIA-expressing (NFIA) cells were quantified. Data are shown as means ± SD. Statistical significance was examined by the Student's t test (**$p < 0.01$).

(D) E11.5 NPCs were infected with GFP control (pMY) and GFP-NFIA-expressing (NFIA) retroviruses, and cultured for 4 days with bFGF. After cell sorting based on GFP fluorescence, genomic DNA was extracted, and the methylation status of the STAT3 binding site in the *gfap* promoter was examined by bisulfite sequencing. Closed and open circles indicate methylated and unmethylated CpG sites, respectively.

(E) Methylation frequency of the CpG site within the STAT3 binding sequence in the *gfap* promoter. Data are shown as means ± SD (N = 3). Statistical significance was examined by the Student t test (*$p < 0.05$).

(F) ChIP assay with a specific antibody for DNMT1 from GFP- and GFP-NFIA-expressing retrovirus-infected NPCs, cultured as in Figure 1G.

(G) E11.5 NPCs were infected with control and DN-NFIA-expressing lentiviruses, and cultured for 4 days with (JAG1-Fc) or without (CTRL) JAG1-Fc in the presence of bFGF. A ChIP assay was performed with a specific antibody for DNMT1 from control (Vehicle) and DN-NFIA-expressing (DN-NFIA) lentivirus-infected NPCs, cultured as in Figure 5F. For quantification, real-time PCR results using specific primers for the *gfap* promoter were indicated as the relative enrichment of DNMT1 compared with NPCs cultured without JAG1-Fc. Data are shown as means ± SD (N = 3). Statistical significance was evaluated by the Student t test (**$p < 0.01$).

retroviruses engineered to express NFIA, and cultured in the presence of LIF. A dramatic induction of GFAP-positive astrocytic differentiation ensued (Figures 5A–5C). As was the case for NICD, GFAP was not expressed in control or NFIA-expressing NPCs in the absence of LIF (data not shown). Furthermore, *gfap* promoter demethylation and DNMT1 dissociation from the promoter were both accelerated in NFIA-expressing NPCs (Figures 5D–5F), as they were in NICD-expressing NPCs. These results prompted us to hypothesize that NFIA is necessary for the Notch-induced dissociation of DNMT1 from the *gfap* promoter. To answer this question, control and dominant-negative NFIA (DN-NFIA)-expressing lentivirus-infected E11.5 NPCs were cultured with JAG1-Fc, a soluble form of the Notch ligand JAG1, for 4 days. We then performed ChIP assays to examine the association of DNMT1 with the *gfap* promoter. In control NPCs, JAG1-Fc treatment led to the dissociation of DNMT1 from the *gfap* promoter, as in the case of NICD expression (Figure 5G). In contrast, we found that dissociation was virtually inhibited in NPCs infected with DN-NFIA-expressing lentiviruses (Figure 5G). Thus, these results indicate that NFIA is prerequisite for the Notch-induced dissociation of DNMT1 from the *gfap* promoter in NPCs. It is noteworthy that a consensus NFI binding site is also present in the promoters of other astrocytic genes, including *S100β*, *aquaporin4*, and *clusterin* (Saadoun et al., 2005; Bachoo et al., 2004) (Figure S8A), and the anticipated binding of NFI to these promoter regions was indeed observed in NICD-expressing NPCs (Figure S8B). Furthermore, demethylation of particular CpG sites within the three promoters was induced in NFIA-expressing NPCs (Figures S9A–S9C). These findings suggest that NFIA acts as a critical molecule downstream of the Notch signaling pathway to potentiate astrocytic differentiation of midgestational NPCs.

NFIA Is Necessary and Sufficient for NPCs to Acquire Astrocytic Potential In Vivo

Finally, we asked whether NFIA indeed plays a critical role in the acquisition of astrocytic potential by NPCs in vivo. To this end, we first stimulated E14.5 NPCs from WT and NFIA-deficient mice with LIF to induce astrocyte differentiation. Since E14.5 NPCs have normally already gained the potential to become

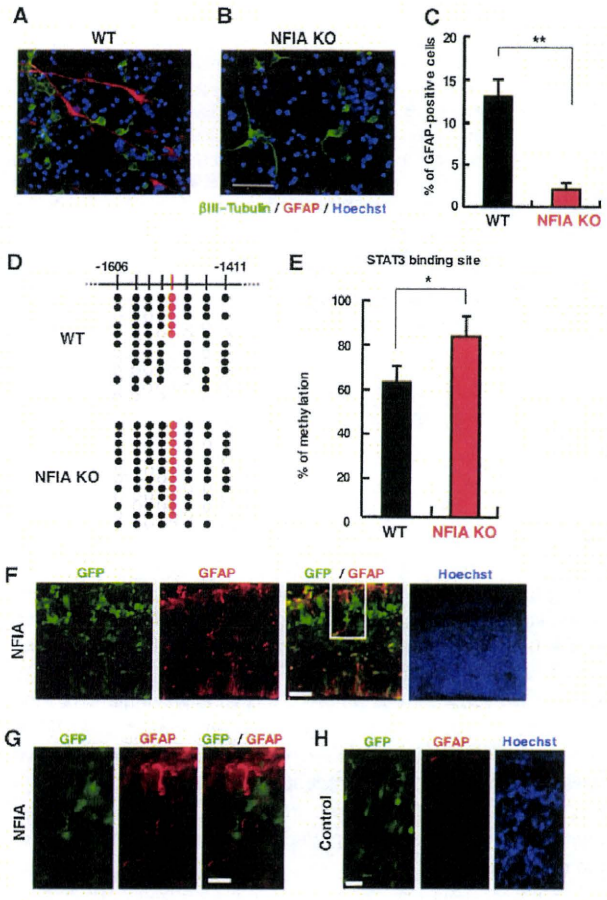

Figure 6. NFIA Is Necessary and Sufficient for the Expression of Astrocytic Potential by NPCs In Vivo

(A and B) NPCs prepared from E14.5 WT (A) or NFIA-deficient (NFIA-KO [B]) mouse telencephalons cultured in the presence of LIF (80 ng/ml) for 4 days to induce astrocytic differentiation. The cells were stained with antibodies against βIII-Tubulin (green) and GFAP (red), and with H33258 to identify nuclei (blue). Scale bar = 50 μm.

(C) GFAP-positive astrocytes in total cells were quantified. Data are shown as means ± SD (n = 3). Statistical significance was evaluated by the Student t test (**$p < 0.01$).

(D) Bisulfite sequencing results for the CpG site within the STAT3 recognition sequence (red) and other CpG sites around this sequence of the *gfap* promoter in telencephalon of WT or NFIA-deficient (NFIA-KO) mouse embryos. Closed and open circles indicate methylated and unmethylated CpG sites, respectively.

(E) Methylation frequency of the CpG site within the STAT3 binding sequence in the *gfap* promoter. Data are shown as means ± SD (n = 3). Statistical significance was examined by the Student t test (*$p < 0.05$).

(F–H) E14.5 forebrain sections of mice expressing GFP (H) and NFIA-GFP (F and G) from plasmids introduced by exo utero electroporation at E11.5 were stained with antibodies against GFP (green) and GFAP (red). Scale bars indicate 50 μm (F) or 20 μm (G and H). (G) High-magnification view of boxed area in (F). Hoechst staining indicates nuclei (blue).

GFAP-positive astrocytes in response to LIF, we observed astrocyte differentiation in the WT NPC culture. In marked contrast, almost no GFAP-positive cells were observed in NFIA-deficient NPCs. Moreover, the *gfap* promoter was significantly more highly methylated in E14.5 NFIA-deficient telencephalons than it was in those of WT litters (Figures 6D and 6E), even though Notch signal was clearly activated in the NFIA-deficient brain (Figure S10). These results indicate that NFIA is indispensable for the Notch signal-induced demethylation of astrocytic gene promoters during brain development.

Using exo utero electroporation, we next examined whether NFIA expression is sufficient for the induction of astrocyte differentiation in the telencephalon. Misexpression of NFIA in E11.5 telencephalon led to precocious generation of GFAP-positive cells at E14.5 (Figures 6F and 6G), indicating that NFIA is sufficient for the production of astrocytes from NPCs in vivo. We suggest that NFIA plays a decisive role in the Notch-induced acquisition of astrocytic potential by NPCs.

DISCUSSION

We have shown in the present study that committed neuronal precursors and young neurons derived from NPCs confer astrocytic differentiation potential on remaining NPCs through Notch signal-induced demethylation of astrocyte-specific gene promoters (Figure 7). The demethylation process is mediated by Notch-induced NFIA, the binding of which to astrocytic gene promoters leads to dissociation of DNMT1 from the promoters. This does not imply that the activation of Notch signaling alone is sufficient for NPCs to differentiate into astrocytes. It potentiates the process, but signals from astrocyte-inducing cytokines are still required to induce differentiation. All members of the IL-6 cytokine family, to which LIF and CT-1 belong, induce GFAP-positive astrocytic differentiation of NPCs by activating STAT1 and/or STAT3 (He et al., 2005; Barnabe-Heider et al., 2005). However, since STAT1 and STAT3 are not capable of binding to methylated cognate sequences (Fan et al., 2005; Takizawa et al., 2001), astrocyte-specific gene promoters must first become demethylated to enable IL-6 cytokines to induce differentiation.

Here, we have shown that committed neuronal precursors and young neurons pregenerated from NPCs express Notch ligands, and provide a feedback signal to Notch-expressing residual NPCs, to acquire astrocyte differentiation potential. In this context, Yoon et al. (2008) have shown recently that the expression of *Dll1* and its critical regulator, *Mindbomb*-1 (*Mib-1*), is restricted to migrating premature neurons and newborn neurons, and that *Mib-1*-expressing neuronal daughters transmit the Notch signal to neighboring NPCs. Moreover, *Mib-1* conditional mutant mice display a complete abrogation of Notch activation, which leads to impairment of NPC maintenance. Together with our results, these data suggest that Notch ligand-expressing, neuronally committed cells are an important cellular source of the Notch signal in development. Such a mechanism would provide an unanticipated level of crosstalk between these different developing cellular populations, and ensure that astrocytes begin to appear only after sufficient numbers of neurons have been generated.

Although Notch signaling clearly enhances astrocyte differentiation, the molecular mechanisms by which it activates glial gene expression have been far from clear. Our results suggest that NFI is one of the downstream target genes of the Notch signaling pathway, and plays a critical role in the Notch-induced

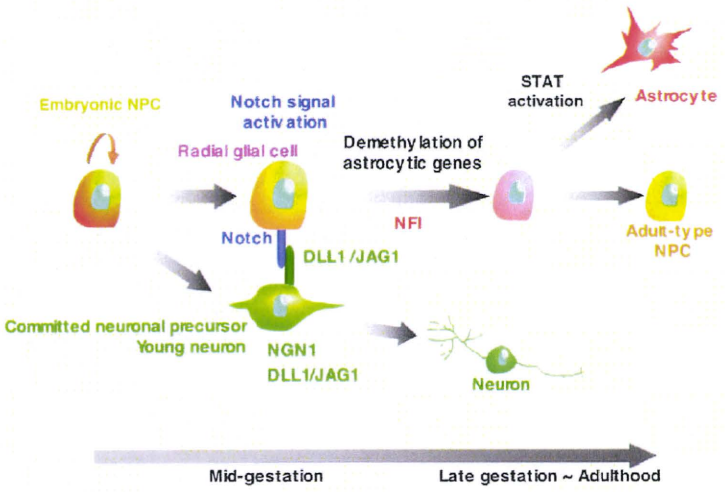

Figure 7. Schematic Representation of Notch Activation-Induced Potentiation of NPCs to Differentiate into Astrocytes and Sequential Changes in the Differentiation Potential of NPCs during Brain Development

At midgestation, an NPC divides asymmetrically and generates a committed neuronal precursor and another NPC (radial glial cells). The committed neuronal precursors and young neurons express Notch ligands and activate Notch signaling in neighboring NPCs, conferring astrocytic differentiation potential on NPCs through NFI expression, which leads to demethylation of astrocyte-specific gene promoters. When the NPCs receive a STAT-activating signal, they differentiate into astrocytes at late gestation. The NPCs eventually become multipotent adult-type NPCs.

acquisition of astrocyte differentiation potential by NPCs. Binding sites for NFI have indeed been identified, not only in the *gfap* promoter, but also in other astrocyte-specific gene promoters (Bachoo et al., 2004; Bisgrove et al., 2000; Gopalan et al., 2006; Saadoun et al., 2005), and *Nfia*$^{-/-}$ mice show reduced expression of these genes (Wong et al., 2007). It will therefore be intriguing to establish the methylation status of these gene promoters in *Nfia* mutant mice.

Since STAT1 and STAT3 are incapable of binding to methylated cognate sequences (Fan et al., 2005; Takizawa et al., 2001), the *gfap* promoter should already be demethylated in such cells as injury-induced reactive astrocytes, which are competent to express GFAP in response to inflammatory cytokines, including the IL-6 family. The existence of different morphological subtypes of astrocytes, such as fibrous and protoplasmic, has long been recognized, and protoplasmic astrocytes are generally GFAP negative (Vaughn and Pease, 1967; Mori and Leblond, 1969; Raff et al., 1984; Raff, 1989). Therefore, it remains unclear whether all astrocyte subtypes derived from NPCs in various brain regions require the Notch-induced demethylation of the *gfap* promoter reported here to become astrocytes.

Although DNA methyltransferases have been well studied biochemically, the molecular mechanism underlying active DNA demethylation is poorly understood, and the existence of DNA-demethylating enzymes is even debatable. A major outstanding question about the stepwise development of NPCs is how DNA methylation status is modulated to endow these precursor populations with glial competency. In this study, we have shown that demethylation of the *gfap* promoter, and dissociation of DNMT1 from the promoter, is caused by the expression of NICD or NFIA in NPCs in a sequential manner. These results suggest that the binding of NFIA to astrocytic gene promoters in Notch-activated NPCs protects the promoters from DNMT1, and hence that NFI plays a critical regulatory role in the epigenetic switch toward astrocytogenesis. We also suggest that demethylation of the *gfap* promoter is attributable to passive, replication-dependent demethylation. It has been reported previously that disruption of *Dnmt1* in NPCs leads to demethylation of astrocytic gene promoters and precocious astrogliogenesis, which suggests that *Dnmt1* is required for the maintenance methylation of astroglial marker genes in NPCs during the early developmental stage (Fan et al., 2005). Furthermore, virus-derived episomal vectors are demethylated at sites where transcription factors bind with high affinity (Hsieh, 1999; Lin et al., 2000), and replication-dependent demethylation of specific sites in *Xenopus* embryos is strongly stimulated by the transactivation domain of the triggering transcription factor (Matsuo et al., 1998). Thus, it is reasonable to hypothesize that passive demethylation is attributable to transcription factors that mask their cognate sites from DNMT1 action, although these and our findings do not yet permit a precise definition of the mechanism.

In summary, our present study offers a plausible explanation for the transitions that occur during the stepwise process of NPC fate specification, and we have suggested how committed neuronal precursors and young neurons might "unlock" nearby NPCs and allow them to differentiate into the next lineage: astrocytes. The activation of Notch signaling in midgestational NPCs induces demethylation of astrocyte-specific genes. Notch ligands are expressed in committed neuronal precursors and young neurons, and Notch-activated NPCs undergo promoter demethylation and acquire the ability to become astrocytes in response to astrocyte-inducing cytokines.

EXPERIMENTAL PROCEDURES

Cell Culture

E11.5 NPCs and embryonic neurons were cultured as described previously (Takizawa et al., 2001). Briefly, E14.5 cortical cells were cultured with bFGF and cytosine arabinoside for 4 days in the eight well chamber slides (4×10^4 cells per well). E11.5 NPCs labeled with EGFP (4×10^4 cells per well) were cultured with the embryonic neurons prepared as above, or alone (8×10^4 cells per well) in the chamber slides. Culturing of WT and CSL-deficient mESCs and induction of mESC NPCs were conducted as described previously (Shimozaki et al., 2005). To activate the Notch signaling pathway in Figure 5G, we used JAG1-Fc (500 ng/ml; R&D Systems).

Plasmids

To express NICD (Takizawa et al., 2003) and NFIA (Deneen et al., 2006), we used the retroviral vector pMY-IRES-GFP (Kitamura et al., 2003), which contains an IRES-GFP cassette that allows identification of transduced cells.

As DN-NFIA, we used the DNA binding domain of NFIA (NFIA-DBD) cloned by PCR from mNFIA cDNA. The NFIA-DBD was cloned into the lentiviral vector (Lois et al., 2002).

Immunostaining

All antibodies for immunostaining in this study and the procedures are descried in Supplemental Experimental Procedures.

LY411575 γ-Secretase Inhibitor Treatment

Pregnant mice were orally dosed with either 1 mg/kg LY411575 (Hyde et al., 2006) or vehicle (dimethyl sulfoxide in sunflower oil) once a day from 10.5 to 13.5 dpc. Twenty-four hours after the last injection at 13.5 dpc, the embryos at E14.5 were obtained for subsequent immunohistochemical analyses.

Bisulfite Sequencing

Cells expressing GFP alone, or GFP together with NICD or NFIA, were isolated by FACSVantage (BD Biosciences), and their genomic DNAs were then extracted. Bisulfite genomic sequencing was performed essentially, as previously described (Takizawa et al., 2001). Specific DNA fragments were amplified by PCR using primers described previously (Takizawa et al., 2001). The PCR products were cloned into pT7Blue vector (Novagen), and 10–16 clones randomly picked from each of three independent PCR amplifications were sequenced.

ChIP Assay

ChIP assays were performed as described previously (Takizawa et al., 2001). Coimmunoprecipitated DNA was used as a template for PCR with primers, the sequences of which are available upon request. Antibodies used for the ChIP assay were mouse anti-CSL (Institute of Immunology) and rabbit anti-NFI (Santa Cruz Biotechonoly), -DNMT1, -DNMT3a, and -DNMT3b (Abcam).

In Vivo Electroporation

Embryonic exo utero surgery and electroporation were performed as described previously (Muneoka et al., 1986; Saito and Nakatsuji, 2001). DNA solutions (pMYs or pMYs-*Nfia*, 2 mg/ml in PBS containing FAST Green) were injected into the lateral ventricle of E11.5 telencephalons. Electronic pulses of 28 V (50 ms) were charged six times at 950-ms intervals using a square-pulse electroporator (CUY21EDIT; Nepa Gene Company).

SUPPLEMENTAL DATA

Supplemental Data include Supplemental Experimental Procedures and ten figures and can be found with this article online at http://www.cell.com/developmental-cell/supplemental/S1534-5807(09)00002-1/.

ACKNOWLEDGMENTS

We thank T. Honjo (Kyoto University) for CSL-deficient ES cells, Y.E. Sun (University of California, Los Angeles) for *Dll3* cDNA, T. Kitamura (University of Tokyo) for pMY vector and Plat-E cells, and F.H. Gage (Salk Institute) for the SOX2-EGFP mouse. We appreciate Y. Bessho and T. Matsui for valuable discussions. We wish to thank the members of our laboratories, in particular I. Nobuhisa, for technical suggestions. We also thank I. Smith for helpful comments and critical reading of the manuscript. We are very grateful to M. Ueda for excellent secretarial assistance. Many thanks to N. Namihira for technical help. This work has been supported by a Grant-in-Aid for Young Scientists, a Grant-in-Aid for Scientific Research on priority areas, the NAIST Global COE Program (Frontier Biosciences: Strategies for Survival and Adaptation in a Changing Global Environment), Kumamoto University COE Program (Cell Fate Regulation Research and Education Unit) from the Ministry of Education, Culture, Sports, Science, and Technology (MEXT) of Japan, by CREST from Japan Science and Technology Agency, and by the Nakajima Foundation and the Uehara Memorial Foundation.

Received: June 30, 2008
Revised: December 1, 2008
Accepted: December 30, 2008
Published: February 16, 2009

REFERENCES

Androutsellis-Theotokis, A., Leker, R.R., Soldner, F., Hoeppner, D.J., Ravin, R., Poser, S.W., Rueger, M.A., Bae, S.K., Kittappa, R., and McKay, R.D. (2006). Notch signalling regulates stem cell numbers in vitro and in vivo. Nature *442*, 823–826.

Bachoo, R.M., Kim, R.S., Ligon, K.L., Maher, E.A., Brennan, C., Billings, N., Chan, S., Li, C., Rowitch, D.H., Wong, W.H., and DePinho, R.A. (2004). Molecular diversity of astrocytes with implications for neurological disorders. Proc. Natl. Acad. Sci. USA *101*, 8384–8389.

Barnabe-Heider, F., Wasylnka, J.A., Fernandes, K.J., Porsche, C., Sendtner, M., Kaplan, D.R., and Miller, F.D. (2005). Evidence that embryonic neurons regulate the onset of cortical gliogenesis via cardiotrophin-1. Neuron *48*, 253–265.

Bertrand, N., Castro, D.S., and Guillemot, F. (2002). Proneural genes and the specification of neural cell types. Nat. Rev. Neurosci. *3*, 517–530.

Bisgrove, D.A., Monckton, E.A., Packer, M., and Godbout, R. (2000). Regulation of brain fatty acid-binding protein expression by differential phosphorylation of nuclear factor I in malignant glioma cell lines. J. Biol. Chem. *275*, 30668–30676.

Campos, L.S., Duarte, A.J., Branco, T., and Henrique, D. (2001). mDll1 and mDll3 expression in the developing mouse brain: role in the establishment of the early cortex. J. Neurosci. Res. *64*, 590–598.

Castro, D.S., Skowronska-Krawczyk, D., Armant, O., Donaldson, I.J., Parras, C., Hunt, C., Critchley, J.A., Nguyen, L., Gossler, A., Gottgens, B., et al. (2006). Proneural bHLH and Brn proteins coregulate a neurogenic program through cooperative binding to a conserved DNA motif. Dev. Cell *11*, 831–844.

Cebolla, B., and Vallejo, M. (2006). Nuclear factor-I regulates glial fibrillary acidic protein gene expression in astrocytes differentiated from cortical precursor cells. J. Neurochem. *97*, 1057–1070.

das Neves, L., Duchala, C.S., Tolentino-Silva, F., Haxhiu, M.A., Colmenares, C., Macklin, W.B., Campbell, C.E., Butz, K.G., and Gronostajski, R.M. (1999). Disruption of the murine nuclear factor I-A gene (Nfia) results in perinatal lethality, hydrocephalus, and agenesis of the corpus callosum. Proc. Natl. Acad. Sci. USA *96*, 11946–11951.

D'Amour, K.A., and Gage, F.H. (2003). Genetic and functional differences between multipotent neural and pluripotent embryonic stem cells. Proc. Natl. Acad. Sci. USA *100* (*Suppl 1*), 11866–11872.

Deneen, B., Ho, R., Lukaszewicz, A., Hochstim, C.J., Gronostajski, R.M., and Anderson, D.J. (2006). The transcription factor NFIA controls the onset of gliogenesis in the developing spinal cord. Neuron *52*, 953–968.

Fan, G., Martinowich, K., Chin, M.H., He, F., Fouse, S.D., Hutnick, L., Hattori, D., Ge, W., Shen, Y., Wu, H., et al. (2005). DNA methylation controls the timing of astrogliogenesis through regulation of JAK-STAT signaling. Development *132*, 3345–3356.

Gopalan, S.M., Wilczynska, K.M., Konik, B.S., Bryan, L., and Kordula, T. (2006). Nuclear factor-1-X regulates astrocyte-specific expression of the alpha1-antichymotrypsin and glial fibrillary acidic protein genes. J. Biol. Chem. *281*, 13126–13133.

Grandbarbe, L., Bouissac, J., Rand, M., Hrabe de Angelis, M., Artavanis-Tsakonas, S., and Mohier, E. (2003). Delta-Notch signaling controls the generation of neurons/glia from neural stem cells in a stepwise process. Development *130*, 1391–1402.

Gronostajski, R.M. (2000). Roles of the NFI/CTF gene family in transcription and development. Gene *249*, 31–45.

He, F., Ge, W., Martinowich, K., Becker-Catania, S., Coskun, V., Zhu, W., Wu, H., Castro, D., Guillemot, F., Fan, G., et al. (2005). A positive autoregulatory loop of Jak-STAT signaling controls the onset of astrogliogenesis. Nat. Neurosci. *8*, 616–625.

Henrique, D., Adam, J., Myat, A., Chitnis, A., Lewis, J., and Ish-Horowicz, D. (1995). Expression of a delta homologue in prospective neurons in the chick. Nature *375*, 787–790.

Hsieh, C.L. (1999). Evidence that protein binding specifies sites of DNA demethylation. Mol. Cell. Biol. *19*, 46–56.

Hyde, L.A., McHugh, N.A., Chen, J., Zhang, Q., Manfra, D., Nomeir, A.A., Josien, H., Bara, T., Clader, J.W., Zhang, L., et al. (2006). Studies to investigate the in vivo therapeutic window of the gamma-secretase inhibitor N2-[(2S)-2-(3,5-difluorophenyl)-2-hydroxyethanoyl]-N1-[(7S)-5-methyl-6-oxo-6,7-dihydro-5H-dibenzo[b,d]azepin-7-yl]-L-alaninamide (LY411,575) in the CRND8 mouse. J. Pharmacol. Exp. Ther. *319*, 1133–1143.

Kato, H., Taniguchi, Y., Kurooka, H., Minoguchi, S., Sakai, T., Nomura-Okazaki, S., Tamura, K., and Honjo, T. (1997). Involvement of RBP-J in biological functions of mouse Notch1 and its derivatives. Development *124*, 4133–4141.

Kawaguchi, A., Ikawa, T., Kasukawa, T., Ueda, H.R., Kurimoto, K., Saitou, M., and Matsuzaki, F. (2008). Single-cell gene profiling defines differential progenitor subclasses in mammalian neurogenesis. Development *135*, 3113–3124.

Kitamura, T., Koshino, Y., Shibata, F., Oki, T., Nakajima, H., Nosaka, T., and Kumagai, H. (2003). Retrovirus-mediated gene transfer and expression cloning: powerful tools in functional genomics. Exp. Hematol. *31*, 1007–1014.

Kohyama, J., Tokunaga, A., Fujita, Y., Miyoshi, H., Nagai, T., Miyawaki, A., Nakao, K., Matsuzaki, Y., and Okano, H. (2005). Visualization of spatiotemporal activation of Notch signaling: live monitoring and significance in neural development. Dev. Biol. *286*, 311–325.

Krohn, K., Rozovsky, I., Wals, P., Teter, B., Anderson, C.P., and Finch, C.E. (1999). Glial fibrillary acidic protein transcription responses to transforming growth factor-beta1 and interleukin-1beta are mediated by a nuclear factor-1-like site in the near-upstream promoter. J. Neurochem. *72*, 1353–1361.

Ladi, E., Nichols, J.T., Ge, W., Miyamoto, A., Yao, C., Yang, L.T., Boulter, J., Sun, Y.E., Kintner, C., and Weinmaster, G. (2005). The divergent DSL ligand Dll3 does not activate Notch signaling but cell autonomously attenuates signaling induced by other DSL ligands. J. Cell Biol. *170*, 983–992.

Lin, I.G., Tomzynski, T.J., Ou, Q., and Hsieh, C.L. (2000). Modulation of DNA binding protein affinity directly affects target site demethylation. Mol. Cell. Biol. *20*, 2343–2349.

Lois, C., Hong, E.J., Pease, S., Brown, E.J., and Baltimore, D. (2002). Germline transmission and tissue-specific expression of transgenes delivered by lentiviral vectors. Science *295*, 868–872.

Louvi, A., and Artavanis-Tsakonas, S. (2006). Notch signalling in vertebrate neural development. Nat. Rev. Neurosci. *7*, 93–102.

Lowell, S., Benchoua, A., Heavey, B., and Smith, A.G. (2006). Notch promotes neural lineage entry by pluripotent embryonic stem cells. PLoS Biol. *4*, e121.

Matsuo, K., Silke, J., Georgiev, O., Marti, P., Giovannini, N., and Rungger, D. (1998). An embryonic demethylation mechanism involving binding of transcription factors to replicating DNA. EMBO J. *17*, 1446–1453.

Mori, S., and Leblond, C.P. (1969). Electron microscopic features and proliferation of astrocytes in the corpus callosum of the rat. J. Comp. Neurol *137*, 197–225.

Muneoka, K., Wanek, N., and Bryant, S.V. (1986). Mouse embryos develop normally exo utero. J. Exp. Zool. *239*, 289–293.

Nye, J.S., and Kopan, R. (1995). Developmental signaling: vertebrate ligands for Notch. Curr. Biol. *5*, 966–969.

Raff, M.C. (1989). Glial cell diversification in the rat optic nerve. Science *243*, 1450–1455.

Raff, M.C., Abney, E.R., and Miller, R.H. (1984). Two glial cell lineages diverge prenatally in rat optic nerve. Dev. Biol. *106*, 53–60.

Saadoun, S., Papadopoulos, M.C., Watanabe, H., Yan, D., Manley, G.T., and Verkman, A.S. (2005). Involvement of aquaporin-4 in astroglial cell migration and glial scar formation. J. Cell Sci. *118*, 5691–5698.

Saito, T., and Nakatsuji, N. (2001). Efficient gene transfer into the embryonic mouse brain using in vivo electroporation. Dev. Biol. *240*, 237–246.

Schroeder, T., Fraser, S.T., Ogawa, M., Nishikawa, S., Oka, C., Bornkamm, G.W., Honjo, T., and Just, U. (2003). Recombination signal sequence-binding protein Jkappa alters mesodermal cell fate decisions by suppressing cardiomyogenesis. Proc. Natl. Acad. Sci. USA *100*, 4018–4023.

Schuurmans, C., Armant, O., Nieto, M., Stenman, J.M., Britz, O., Klenin, N., Brown, C., Langevin, L.M., Seibt, J., Tang, H., et al. (2004). Sequential phases of cortical specification involve neurogenin-dependent and -independent pathways. EMBO J. *23*, 2892–2902.

Shimozaki, K., Namihira, M., Nakashima, K., and Taga, T. (2005). Stage- and site-specific DNA demethylation during neural cell development from embryonic stem cells. J. Neurochem. *93*, 432–439.

Shu, T., Butz, K.G., Plachez, C., Gronostajski, R.M., and Richards, L.J. (2003). Abnormal development of forebrain midline glia and commissural projections in Nfia knock-out mice. J. Neurosci. *23*, 203–212.

Steele-Perkins, G., Plachez, C., Butz, K.G., Yang, G., Bachurski, C.J., Kinsman, S.L., Litwack, E.D., Richards, L.J., and Gronostajski, R.M. (2005). The transcription factor gene Nfib is essential for both lung maturation and brain development. Mol. Cell. Biol. *25*, 685–698.

Takizawa, T., Nakashima, K., Namihira, M., Ochiai, W., Uemura, A., Yanagisawa, M., Fujita, N., Nakao, M., and Taga, T. (2001). DNA methylation is a critical cell-intrinsic determinant of astrocyte differentiation in the fetal brain. Dev. Cell *1*, 749–758.

Takizawa, T., Ochiai, W., Nakashima, K., and Taga, T. (2003). Enhanced gene activation by Notch and BMP signaling cross-talk. Nucleic Acids Res. *31*, 5723–5731.

Temple, S. (2001). The development of neural stem cells. Nature *414*, 112–117.

Tokunaga, A., Kohyama, J., Yoshida, T., Nakao, K., Sawamoto, K., and Okano, H. (2004). Mapping spatio-temporal activation of Notch signaling during neurogenesis and gliogenesis in the developing mouse brain. J. Neurochem. *90*, 142–154.

Vaughn, J.E., and Pease, D.C. (1967). Electron microscopy of classically stained astrocytes. J. Comp. Neurol. *131*, 143–154.

Weinmaster, G. (1997). The ins and outs of notch signaling. Mol. Cell. Neurosci. *9*, 91–102.

Wong, Y.W., Schulze, C., Streichert, T., Gronostajski, R.M., Schachner, M., and Tilling, T. (2007). Gene expression analysis of nuclear factor I-A deficient mice indicates delayed brain maturation. Genome Biol. *8*, R72.

Xue, Y., Gao, X., Lindsell, C.E., Norton, C.R., Chang, B., Hicks, C., Gendron-Maguire, M., Rand, E.B., Weinmaster, G., and Gridley, T. (1999). Embryonic lethality and vascular defects in mice lacking the Notch ligand Jagged1. Hum. Mol. Genet. *8*, 723–730.

Yoon, K.J., Koo, B.K., Im, S.K., Jeong, H.W., Ghim, J., Kwon, M.C., Moon, J.S., Miyata, T., and Kong, Y.Y. (2008). Mind bomb 1-expressing intermediate progenitors generate notch signaling to maintain radial glial cells. Neuron *58*, 519–531.

Yoshimatsu, T., Kawaguchi, D., Oishi, K., Takeda, K., Akira, S., Masuyama, N., and Gotoh, Y. (2006). Non-cell-autonomous action of STAT3 in maintenance of neural precursor cells in the mouse neocortex. Development *133*, 2553–2563.

Epigenetic regulation of neural cell differentiation plasticity in the adult mammalian brain

Jun Kohyama[a], Takuro Kojima[b,c,d], Eriko Takatsuka[a], Toru Yamashita[b,c], Jun Namiki[b], Jenny Hsieh[e], Fred H. Gage[f], Masakazu Namihira[a], Hideyuki Okano[b], Kazunobu Sawamoto[c,d], and Kinichi Nakashima[a,1]

[a]Laboratory of Molecular Neuroscience, Graduate School of Biological Sciences, Nara Institute of Science and Technology, Nara 630-0101, Japan; [b]Department of Physiology, and [c]Bridgestone Laboratory of Developmental and Regenerative Neurobiology, Keio University School of Medicine, Tokyo 160-8582, Japan; [d]Department of Developmental and Regenerative Biology, Nagoya City University Graduate School of Medical Sciences, 1 Kawasumi, Mizuho-ku, Nagoya 467-8601, Japan; [e]Department of Molecular Biology and Cecil H. and Ida Green Center for Reproductive Biology Sciences, UT Southwestern Medical Center, Dallas, TX 75390; and [f]Laboratory of Genetics, The Salk Institute, La Jolla, CA 92037

Contributed by Fred H. Gage, October 2, 2008 (sent for review July 12, 2008)

Neural stem/progenitor cells (NSCs/NPCs) give rise to neurons, astrocytes, and oligodendrocytes. It has become apparent that intracellular epigenetic modification including DNA methylation, in concert with extracellular cues such as cytokine signaling, is deeply involved in fate specification of NSCs/NPCs by defining cell-type specific gene expression. However, it is still unclear how differentiated neural cells retain their specific attributes by repressing cellular properties characteristic of other lineages. In previous work we have shown that methyl-CpG binding protein transcriptional repressors (MBDs), which are expressed predominantly in neurons in the central nervous system, inhibit astrocyte-specific gene expression by binding to highly methylated regions of their target genes. Here we report that oligodendrocytes, which do not express MBDs, can transdifferentiate into astrocytes both *in vitro* (cytokine stimulation) and *in vivo* (ischemic injury) through the activation of the JAK/STAT signaling pathway. These findings suggest that differentiation plasticity in neural cells is regulated by cell-intrinsic epigenetic mechanisms in collaboration with ambient cell-extrinsic cues.

glia | JAK/STAT

The mammalian cerebral cortex originates from neural stem/neural progenitor cells (NSCs/NPCs), which self-renew and give rise to the three major brain cell types: neurons, astrocytes, and oligodendrocytes (1). The fate of NSCs/NPCs in the developing brain is believed to be determined by external cues that involve various types of cytokines and internal cellular programs (2, 3).

Among the three NSC/NPC progenies, astrocyte differentiation from NSCs/NPCs is largely dependent on the activation of the Janus kinase (JAK)/signal transducer and activator of transcription (STAT) pathway (4, 5). Impairment of astrocyte differentiation in gene knockout mice lacking leukemia inhibitory factor (LIF) (6), LIF receptor β (7), gp130 (8), and STAT3 (9) strongly suggests that the JAK-STAT signaling pathway plays a critical role for astrogliogenesis in the developing central nervous system (CNS).

Cell-intrinsic programs regulating fate determination of NSCs/NPCs include epigenetic modifications such as chromatin remodeling and DNA methylation. The cytosine residue in CpG dinucleotides of vertebrate genomes is a well-known target for DNA methylation, leading to suppression of methylated genes. Establishment of the proper gene methylation patterns is essential for inactivation of the X-chromosome, genomic imprinting, and normal development. Consistently, abnormalities in DNA methylation are associated with tumorigenesis (10) and with several neurological disorders including Rett (RTT), immunodeficiency-centromeric instability-facial anomalies (ICF), fragile-X, and α-thalassemia mental retardation (ATRX) syndromes (11).

Mechanistically, DNA methylation is considered to elicit its effects by interfering with binding of transcriptional factors to their cognate recognition sequences (12) or by creating a binding site for members of a transcriptional repressor family, the methyl-CpG binding proteins (MBDs), that recognize methylated CpG sequences (13).

During development, NSCs/NPCs change their differentiation potential via alternation of epigenetic modification. In early neurogenic period, the fetal NSCs/NPCs are unable to generate astrocytes even when stimulated with known astrocyte-inducing cytokines such as LIF, which activate the JAK/STAT pathway, due to DNA hypermethylation in the promoter regions of astrocytic genes (14, 15). The promoter regions become demethylated as gestation proceeds, conferring astrocyte differentiation potential to NSCs/NPCs in response to astrocyte-inducing cytokines. After CNS development is complete, differentiated cells may still be exposed to a variety of stimuli including physiological and pathological stress: for example, it has been reported that focal cerebral ischemia triggers JAK/STAT activation (16). Meanwhile, it remains unclear how differentiated cells maintain their traits or how their differentiation plasticity is regulated under normal or pathological conditions. There should at least be a mechanism of escaping from pathologic astrogliogenic stimuli on non astrocytic lineages.

In this study, we demonstrate that expression of MBDs is highly relevant to differentiation plasticity against astrocytic stimuli in adult neural cells. Oligodendrocytes which are devoid of MBDs can respond to JAK-STAT pathway activators and differentiate into astrocytes *in vitro*. Ectopic expression of MeCP2, one of the MBDs, in oligodendrocytes can suppress astrocytic differentiation even in the presence of astrocyte-inducing cytokines. By means of oligodendrocyte-fate tracing system, we further show that oligodendrocytes can convert into astrocytic lineages after brain ischemic injury. We thus provide a model in which *in vivo* unexpected cellular differentiation plasticity could contribute to the pathogenesis of injuries in the CNS.

Results

Oligodendrocytes but Not Neurons Have the Capacity to Respond to Astrogliogenic Stimulation. As a first step toward unraveling the mechanisms regulating the cellular identity of differentiated neural cells, we sought to examine whether neurons and oligodendrocytes express a typical astrocytic marker, glial fibrillary acidic protein (GFAP), in response to LIF stimulation. We used adult hippocampus-derived multipotent NPCs (AHPs) to obtain each differentiated cell type (17). When neurons were incubated with LIF for 2 days, no cells were found to be simultaneously positive for both the neuronal marker microtubule-associated protein 2ab (Map2ab) and GFAP (Fig. 1*A*, *Upper*). In this experiment, GFAP-positive cells were most likely to have differentiated from AHPs in response

Author contributions: J.K. and K.N. designed research; J.K., T.K., E.T., T.Y., J.N., and M.N. performed research; K.N. analyzed data; and J.K., J.H., F.H.G., H.O., K.S., and K.N. wrote the paper.

The authors declare no conflict of interest.

[1]To whom correspondence should be addressed. E-mail: kin@bs.naist.jp.

This article contains supporting information online at www.pnas.org/cgi/content/full/0808417105/DCSupplemental.

www.pnas.org/cgi/doi/10.1073/pnas.0808417105

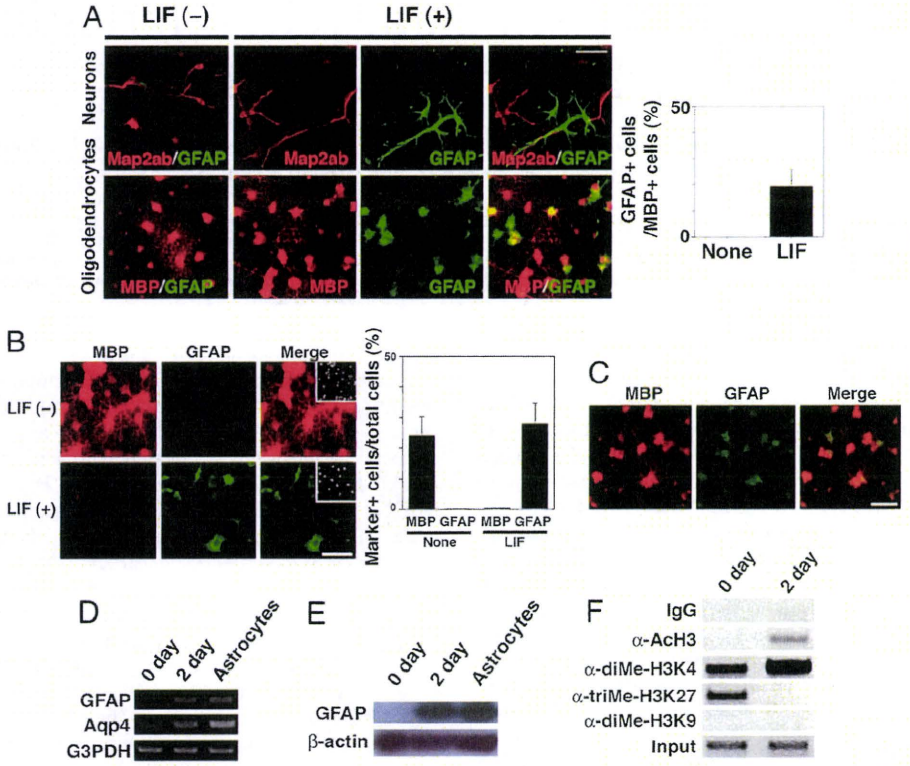

Fig. 1. Differentiation plasticity of oligodendrocytes. (*A*) AHP-derived neurons and oligodendrocytes were cultured for 2 days with or without LIF (50 ng/ml). Cells were then stained with sets of antibodies for Map2ab (*Upper*, red)/GFAP (*Upper*, green) and MBP (*Bottom*, red)/GFAP (*Lower*, green). (Scale bar: 50 μm.) The percentage of GFAP-positive cells in MBP-positive cells was quantified (*Right*). Data are mean ± SD. (*B*) Oligodendrocytes were cultured with or without LIF (50 ng/ml) for 4 days and subsequently stained for MBP (red) and GFAP (green). *Insets*: Hoechst nuclear staining of each field. (Scale bar: 50 μm.) Percentages of MBP- and GFAP-positive cells in total cells were quantified (*Right*). Data are mean ± SD. (*C*) GFAP-positive astrocytes appeared with LIF treatment for 2 days even when the cells were growth-arrested by aphidicolin (10 μg/ml). MBP (red), GFAP (green). (Scale bar: 50 μm.) (*D*) AHP-derived oligodendrocytes (0 day), oligodendrocytes incubated with LIF (50 ng/ml) for 2 days (2 day), and AHP-derived astrocytes were analyzed by RT-PCR using specific sets of primers against *gfap*, *Aqp4* and *G3PDH*. (*E*) AHP-derived oligodendrocytes (0 day), oligodendrocytes incubated with LIF (50 ng/ml) for 2 days (2 day), and AHP-derived astrocytes were analyzed by Western blot using an antibody against GFAP. A band corresponding to the molecular weight of GFAP protein (~50 kDa) was detected. (*F*) Differentiated oligodendrocytes (0 day) were incubated with LIF (50 ng/ml) for 2 days and then subjected to ChIP assay using control IgG, anti-diMe-H3K4, -diMe-H3K9, -triMe-H3K27 and -AcH3 antibodies. Co-immunoprecipitated *gfap* gene fragment (−18bp to + 513bp) was amplified by PCR with a specific set of primers. Nucleotide positions are those of GenBank accession number Z48978.

to LIF stimulation. In contrast, about 20% of cells that were positive for a mature oligodendrocyte marker, myelin basic protein (MBP), also became positive for GFAP in the LIF-stimulated condition, demonstrating their differentiation plasticity (Fig. 1*A*, *Lower* and *Right* graph). We also observed GFAP expression in a significant number of cells that were positive for another oligodendrocyte marker, CNPase [supporting information (SI) Fig. S1]. When we extended culturing with LIF to 4 days, MBP expression almost disappeared and the cells instead became exclusively GFAP-positive (Fig. 1*B*). We obtained similar results using a different astrocyte marker, S100β, with MBP (Fig. S2), and another oligodendrocyte marker, RIP, with GFAP (not shown). These results suggest that oligodendrocytes were converted into GFAP-positive astrocytes. GFAP expression in MBP-positive oligodendrocytes was observed, in the presence of LIF, even after treatment with the DNA polymerase inhibitor aphidicolin to arrest cell division (Fig. 1*C*). By measuring BrdU uptake, we confirmed that the cells were indeed growth-arrested (not shown), which suggests that cell division is dispensable for oligodendrocyte-astrocyte (O-A) conversion.

Oligodendrocyte-Astrocyte Conversion Is Accompanied by Epigenetic Modification Change. We next asked whether a change in chromatin modifications around the *gfap* transcription initiation site in oligodendrocytes occurred during the O-A transition. As shown in Fig. 1*D*, transcription of *gfap* and of another astrocytic marker, *aquaporin4* (Aqp4) (18), was upregulated, and immunoblot analysis (Fig. 1*E*) revealed that GFAP levels were also strikingly higher. Histone H3-lysine 4 (H3K4) methylation and H3 acetylation are consistent markers of transcriptionally active genes, whereas silent genes are marked by increased levels of H3K9 and H3K27 methylation (19). Chromatin immunoprecipitation (ChIP) experiments showed that H3K4 methylation and H3 acetylation increased during the O-A transition (Fig. 1*F*), in agreement with the immunocytochemical data, revealing that the chromatin status of *gfap* was altered toward the active state following LIF stimulation. We could not detect a distinct signal corresponding to H3K9 methylation, which may indicate that *gfap* transcription is poised but not actively suppressed in oligodendrocytes by H3K27 methylation (20). In support of this idea, H3K27 trimethylation on *gfap* was observed before LIF treatment (Fig. 1*F*, 0 day).

Oligodendrocytes Convert into Astrocytes *in Vivo* After Injury. Given that O-A transition was observed *in vitro* when oligodendrocytes were stimulated by astrocyte-inducing cytokine, we then asked whether O-A conversion also occurs *in vivo*. To this end, we specifically labeled oligodendrocytes *in vivo* and traced their fates with the Cre-loxP recombination system (Fig. 2*A* and *B*). We intercrossed two transgenic mouse lines: 1) MBP-Cre-tg (21), in

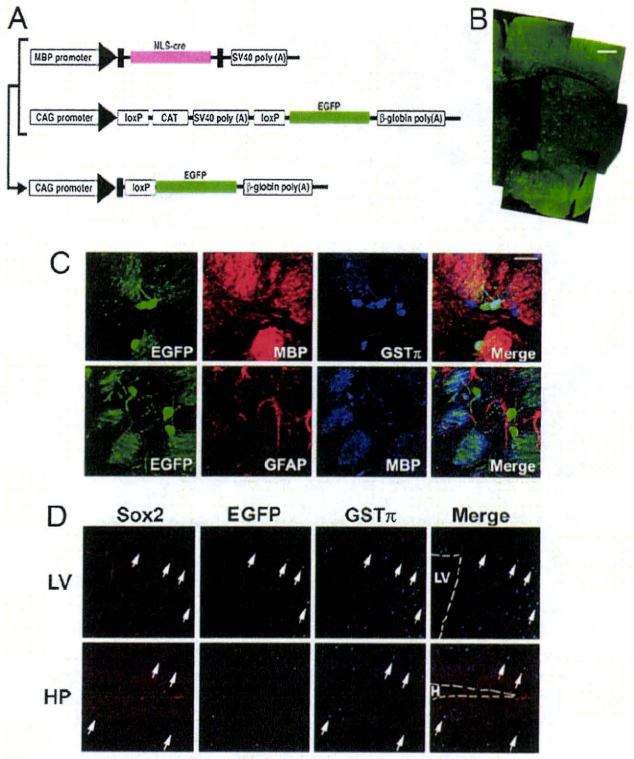

Fig. 2. Oligodendrocyte-specific labeling with EGFP. (*A*) Schematic of transgenic constructs used to trace the lineage of oligodendrocytes. In double-transgenic mice harboring the upper two transgenes, Cre recombinase is expressed in MBP-expressing oligodendrocytes and excises the floxed CAT-SV40 poly(A) fragment, resulting in constitutive expression of EGFP under the control of the ubiquitous CAG promoter. (*B*) Distribution of EGFP-positive cells in the adult brain. (Scale bar: 500 mm.) (*C*) EGFP expression was confined to MBP- and GST-π-positive mature oligodendrocytes in the adult brain under normal conditions (*Upper*). Expression of EGFP and GFAP was mutually exclusive (*Lower*). (Scale bar: 20 μm.) (*D*) Expression of EGFP in neurogenic regions of the adult brain. Arrows indicate representative cells expressing EGFP and the oligodendrocyte marker GST-π. Sox2 expression was not observed in the EGFP-positive cells. LV, lateral ventricle; HP, hippocampus; H, hilus. (Scale bar: 100 mm.)

which Cre recombinase is expressed under the control of the *mbp* promoter, and 2) CAG-CAT-EGFP-tg (22), in which EGFP expression is induced in Cre-expressing cells and their progeny under the control of the ubiquitous CAG promoter. Accordingly, in double-transgenic mice, once cells differentiate into MBP-expressing mature oligodendrocytes, they should sustain EGFP expression irrespective of what cell type they later become. We confirmed the previously determined specificity of the MBP promoter (21), and found that EGFP expression occurred exclusively in MBP-positive oligodendrocytes, but not in other cell types such as GFAP-positive astrocytes, in the adult brain of double-transgenic mice under normal conditions (Fig. 2*C*). The EGFP expression was not observed in a NSC/NPC marker Sox2-positive cells localized in the subventricular zone of the lateral ventricle or the subgranular zone of the hippocampus (Fig. 2*D*). EGFP was not expressed in cells positive for NG2, a marker for immature oligodendrocytes and/or glial progenitors (23) (data not shown). These results suggest that activation of the *mbp* promoter is confined to mature oligodendrocytes.

Because GFAP expression is dramatically induced by CNS injury (24), we subjected the double-transgenic mice to middle cerebral artery occlusion (MCAO) and traced the lineage of EGFP-positive cells. MCAO has been reported to activate the JAK/STAT pathway, as is the case with LIF stimulation (16). Consistent with the previous finding, we indeed detected STAT3 activation in oligodendrocytes after MCAO injury (Fig. 3*A*). Cells positive for both EGFP and phosphorylated STAT3 seemed to retain oligodendrocytic characteristics as judged by oligodendrocyte-specific marker expression 3 days after MCAO (Fig. 3*B*). Two weeks after surgery, we found that significant numbers of EGFP-positive cells became GFAP-positive astrocytes in and around the infarct area (Fig. 3 *C* and *D*), but not in unlesioned areas. Almost all other EGFP-positive/GFAP-negative cells still expressed MBP and appeared to retain oligodendrocytic characteristics (Fig. S3). We found no evidence for BrdU uptake in EGFP-positive cells after MCAO, probably because they did not divide during the O-A transition (Fig. S4). EGFP and GFAP double-positive cells were negative for cleaved caspase 3, indicating that they were not apoptotic (Fig. S5). Although one might argue that the *mbp* promoter was ectopically *trans*-activated in these GFAP-expressing astrocytes after injury, we could not detect EGFP expression in cultured astrocytes derived from adult MBP-cre/EGFP mice even when the cells were stimulated with LIF (Fig. 3*E*). Furthermore, the possibility that EGFP-positive cells de-differentiated into NSCs/NPCs is unlikely, because we could not detect ectopic or re-expression of the NSC/NPC neural marker Sox2 in these cells after injury (Fig. S6). Moreover, EGFP-positive cells also became GFAP-positive when the transgenic mice were subjected to another injury model, cold injury (Fig. S7), implying that the O-A transition occurs after diverse types of brain injury.

Neuron-Specific Expression of Methyl CpG Binding Proteins (MBDs) in CNS. Because epigenetic modification is known to be critically involved in defining cell-typespecific gene expression, we hypothesized that an epigenetic mechanism could be responsible for the differentiation plasticity of these neural cells. We therefore examined the DNA methylation status of *gfap* in each neural cell type derived from adult AHPs by the bisulfite sequencing method (Fig. 4*A*) and found that the *gfap* promoter region around the STAT3 binding site was completely unmethylated, whereas the region around the transcriptional start site was extensively methylated, in all of the neural cell types. Next, we examined the expression of MeCP2, a member of the MBD family, because we have recently reported that MBDs play an important role in restricting astrocyte-specific gene expression in neurons that have differentiated from fetal NPCs (25). Representative brain sections stained with antibodies against MeCP2 and against markers of neurons (NeuN), oligodendrocytes (GST-π) and astrocytes (S100β) are shown in Fig. 4 *B* and *C*. In oligodendrocyte fate-tracing mice, as mentioned above, MeCP2 expression was not observed in oligodendrocytes that were labeled by EGFP (Fig. 4*D*). These results are consistent with previous reports that MBDs are expressed predominantly in neurons, and not in glial cells, in the CNS (26). Neurons, but not oligodendrocytes or astrocytes, that have differentiated from AHPs *in vitro* also express MeCP2 (Fig. 4*E*). As has been observed for fetal NSCs/NPCs and cells differentiated from them (25), we found that in all neural cell types derived from AHPs the region around the *gfap* transcription initiation site was extensively methylated (Fig. 4*A*), suggesting that this region is a target for MBD binding in cells expressing MBDs (26) (Fig. 4*D*) to suppress *gfap* expression. Furthermore, we also found that another MBD, MBD1, shows a quite similar distribution to MeCP2 in adult brain (Fig. 4*F*).

MeCP2 Is Sufficient to Restrict Astrocytic Gene Expression. In light of the above findings, we examined the function of MeCP2 in terms of astrocytic differentiation of cells that are competent for LIF stimulation, i.e., NSCs/NPCs and oligodendrocytes. AHPs, which normally express GFAP in response to LIF, were transduced with recombinant retroviruses engineered to express EGFP (control) or both EGFP and MeCP2. In AHPs, the ectopic expression of MeCP2 led to suppression of astrocytic fate, consistent with our previous observation in fetal NSCs/NPCs (Fig. 5*A* and *B*). Next, to examine the possibility that the O-A conversion potential of oligo-

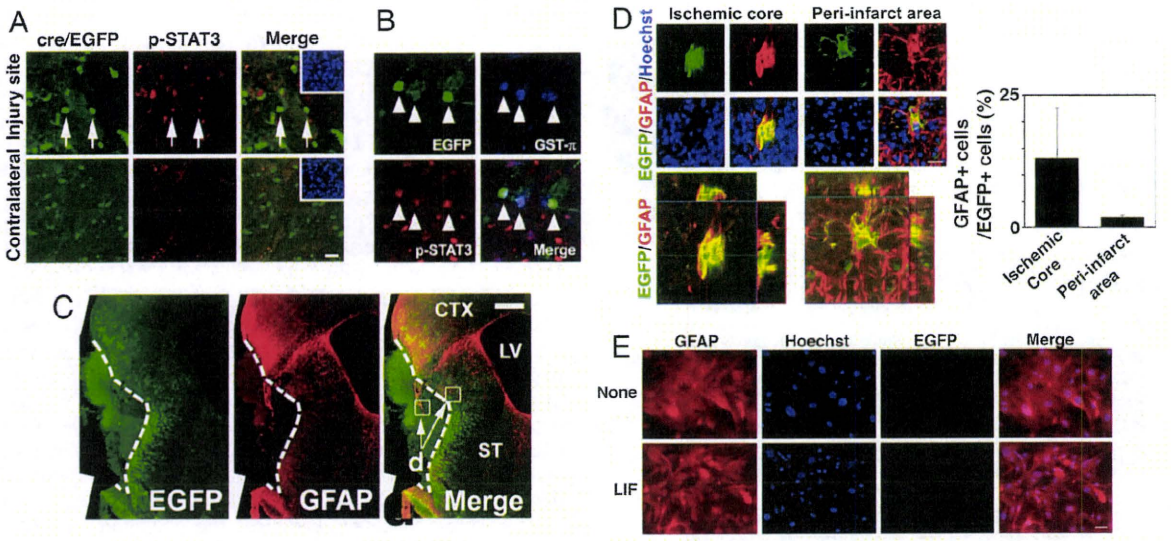

Fig. 3. STAT activation and O-A conversion after ischemic injury. (*A*) Activation of the JAK/STAT pathway in EGFP-positive cells was evaluated by immunostaining using an antibody against phospo-STAT3 (*p*-STAT3) in the injured and contralateral sides of the striata 72 h after ischemic injury. Arrows indicate representative cells positive for both EGFP and *p*-STAT3. (Scale bar: 20 μm.) *Insets*: Hoechst nuclear staining of each field. (*B*) *p*-STAT3 was also detected in GST-π-expressing EGFP-positive cells 72 h after injury (arrowheads). (Scale bar: 20 μm.) (*C*) A representative brain section stained with anti-GFP and -GFAP antibodies 2 weeks after MCAO surgery. Scale bar = 500 μm. CTX, cortex; CC, corpus callosum; LV, lateral ventricle; ST, striatum. (*D*) Higher magnification views of square areas in *C*. GFAP expression appeared in EGFP-expressing cells in the ischemic core (*Left* square arrowed in *C*, *Upper Left*) and peri-infarct (*Right* square arrowed in *C*, *Upper Right*) areas. Representative cells positive for both GFAP and EGFP are shown; *Lower Right* image in each group is a superimposition of the other three images. (Scale bar: 20 μm.) Three-dimensional digital images of each area are also shown (ischemic core area, *Bottom Left*; peri-infarct area, *Bottom Right*). Percentage of GFAP-positive cells in EGFP-positive cells was quantified for each area (graph). Data are mean ± SD. (*E*) Astrocytes prepared from adult MBP-Cre/EGFP transgenic mice were left untreated or treated with LIF for 4 days, and then stained for EGFP (green) and GFAP (red). (Scale bar: 50 μm.) EGFP expression was not induced even when the cells were stimulated with LIF.

dendrocytes might be attributable to the lack of MBD expression, we transfected AHPs with MBP-Cre vector and control floxed neo or floxed neo-MeCP2-expressing vector together with floxed CAT-EGFP-expressing vector, and subsequently differentiated them into oligodendrocytes, then stimulated with LIF for 4 days. As shown in Fig. 5*C*, GFAP and S100β expression was clearly inhibited by the expression of MeCP2 in oligodendrocytes.

Discussion

It has become increasingly evident that a dynamic interplay between cellular extrinsic cues and cell intrinsic programs plays important roles in the fate determination of NSCs/NPCs. Among cell internal programs, epigenetic modification, especially DNA methylation, is important for acquisition of astrocyte-differentiation potential in NCSs/NPCs. In this work, we have shown that DNA methylation plays a critical role in restricting astrocytic property in neural cells in concert with MBDs. Notably, the astrocyte differentiation potential of oligodendrocytes may be attributable to loss of DNA methylation in the promoter regions of astrocytic genes and undetectable expression of MBDs. We have shown that oligodendrocytes derived from adult AHPs can respond to an astrocyte-inducing cytokine to become GFAP-positive astrocytes (Fig. 1). We further demonstrate that oligodendrocytes can also convert to GFAP-positive astrocytes after ischemic injury (Fig. 2), although because we have not examined functional maturation of the oligodendrocyte-derived astrocytes, this point will need to be addressed further in a future study.

Regarding cell plasticity, we have previously shown that even adult NSCs/NPCs retain substantial differentiation plasticity depending on the surrounding milieu (27). Ectopic expression of the proneural gene *ascl* (also known as *mash1*) induces oligodendrocyte differentiation of NSCs/NPCs located in one of the major neurogenic regions in the adult brain (the granular layer of the hippocampus), whereas it induces neuronal differentiation of NSCs/NPCs in another neurogenic region (the subventricular zone) and in *in vitro* culture conditions. Thus, it is becoming apparent that cells are more plastic than had previously been thought.

Our present study provides a molecular mechanism whereby cells can regulate their identity by repressing genes that are expressed in other lineages. Such an expression selectivity or exclusiveness of cell-type specific gene has been extensively examined in a series of studies of transcriptional repressor element1-silencing transcription factor (REST)/neuron-restrictive silencer factor (NRSF) (28). REST/NRSF suppresses neuronal gene expression in non-neural tissues to establish non-neuronal identity. Consistently REST/NRSF is expressed in non-neural tissues and dysfunction of REST/NRSF leads to ectopic neuronal gene expression in non-neural tissues. In contrast to the function of REST/NRSF, MBDs are expressed selectively in neurons in the CNS and repress glial genes (Figs. 4 and 5). We have previously shown by ChIP assay that MeCP2 binds to the highly methylated region of *gfap* in neurons that are expressing MeCP2 (25). MeCP2 deficiency in neurons may therefore lead to expression of genes that are normally astrocyte-specific. Indeed, many glial gene transcripts, including *gfap*, were found to be up-regulated in the brains of Rett syndrome patients with a mutation in *mecp2* (29). However, no major phenotype related to cellular differentiation in MeCP2-deficient mice is known, probably due to functional redundancy and overlapping expression among MBDs (25) (Fig. 4*F*). To address this point more precisely, we must await future studies in mice with compound disruption of several MBD genes.

It has long been thought that, after CNS injury, oligodendrocytes can only die, which could explain subsequent demyelination (30). However, we have shown here that significant numbers of oligodendrocytes actually become GFAP-positive cells following injury, suggesting that O-A conversion may be in part responsible for postinjury demyelination; oligodendrocytes may instead provide a source of newly generated GFAP-positive astrocytes in damaged nervous systems *in vivo*. Although astrocytes form a glial scar and are considered to be detrimental for axonal regeneration in the

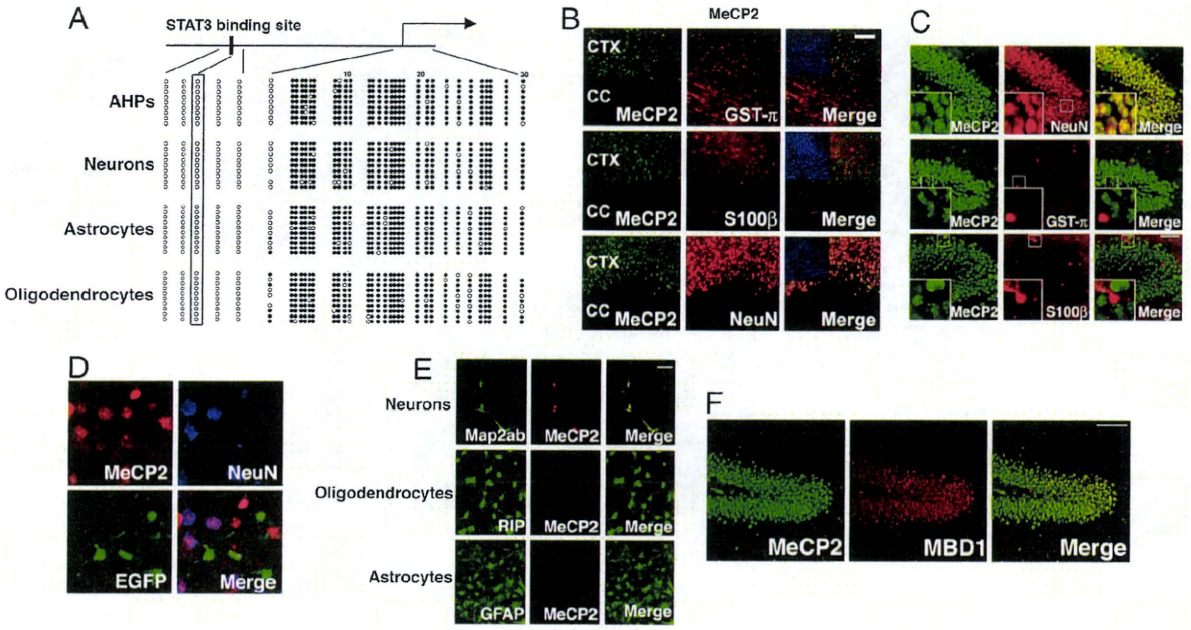

Fig. 4. MeCP2 is predominantly expressed in neurons and suppresses astrocytic gene expression in oligodendrocytes when ectopically expressed. (*A*) Schematic representation of *gfap* locus (*Upper*). Methylation status of five CpG sites around the STAT3 binding site (black box), which is critical for LIF-induced activation of the *gfap* promoter, and of 30 CpG sites around the transcription initiation site (arrow) were examined for each cell type by bisulfite sequencing. Open and closed circles indicate unmethylated and methylated CpG sites, respectively. (*B*) MeCP2 expression (green) was examined in adult mouse brain sections. Neurons, oligodendrocytes, and astrocytes are identified with specific antibodies for NeuN (red, *Upper* middle), GST-π (red, center), and S100β (red, *Lower* middle), respectively. Staining of the hippocampal dentate gyrus region is shown. *Insets*: higher magnification views of square areas in each field. (Scale bar: 50 μm.) (*C*) MeCP2 is predominantly expressed in neurons. MeCP2 expression (green) was examined in the adult mouse cortex and corpus callosum. Oligodendrocytes, astrocytes, and neurons were identified with specific antibodies for GST-π (red, *Upper* rows), S100β (red, middle rows), and NeuN (red, *Bottom* rows), respectively. *Insets*: Hoechst nuclear images of each field. (Scale bar: 100 μm.) CTX, cortex; CC, corpus callosum. (*D*) EGFP-positive cells do not express MeCP2. MeCP2 expression (*Upper Left*) was observed in NeuN-positive (*Upper Right*) but not in EGFP-positive (*Lower Left*) cells. (*E*) MeCP2 (red) is expressed in Map2ab-positive neurons (*Top*, green), but not in RIP-positive oligodendrocytes (middle, green) or GFAP-positive astrocytes (*Bottom*, green) generated from AHPs *in vitro*. (Scale bar: 50 μm.) (*F*) Redundant expression of MBDs *in vivo*. Expression of MeCP2 (green, *Left*) and MBD1 (red, middle), another member of the MBD family, was examined in the adult hippocampal region. These two MBDs showed the same expression pattern (*Right*). (Scale bar: 100 μm.)

injured CNS, it has been recently demonstrated that astrocytes also play a crucial role in wound healing and functional recovery in the subacute phase of spinal cord injury (31). During this phase, astrocytes migrate to compact the lesion, presumably excluding the inflammatory cells to prevent them from spreading in the parenchyma of the spinal cord. Assuming that astrocytes in the brain function as do those in the spinal cord, the oligodendrocyte-to-astrocyte conversion may contribute to an increase in the number of astrocytes after injury in the brain as well. We have also proposed an epigenetic mechanism to explain this differentiation plasticity of oligodendrocytes. To better understand how the injured brain might recover by shifting its cellular profile (e.g., from oligodendrocytes to astrocytes), this study emphasizes the need to consider both cell-intrinsic processes and cell-extrinsic cues. We suggest that epigenetic factors such as MBD proteins play important roles in the maintenance of cellular homeostasis after injury, providing a built-in system to relay signals from an ever-changing environment to the neural cell genome.

Materials and Methods

Cell Culture and *in Vitro* Differentiation. Neural progenitor cells (AHPs) isolated from hippocampus of adult female Fischer 344 rats, used in this study, have been characterized previously (32). The methods for maintaining AHPs and inducing their differentiation into specific lineages have been reported (17). For a detailed description, see *SI Text*.

Reverse TranscriptionPolymerase Chain Reaction. RNA isolation and reverse transcriptionpolymerase chain reaction (RT-PCR) were performed by an established method.

For a detailed description, see *SI Text*.

Western Blot Analysis. Western blot analysis was performed by an established method.

For a detailed description, see *SI Text*.

Immunostaining. Cells were fixed with 4% paraformaldehyde (PFA) and stained immunocytochemically, as described previously (25). For a detailed description, see *SI Text*.

Recombinant Retrovirus. Retrovirus was produced as previously described (33). For a detailed description, see *SI Text*.

Bisulfite Sequencing. Sodium bisulfite treatment of genomic DNA was performed essentially as described previously (34). For a detailed description, see *SI Text*.

Chromatin Immunoprecipitation Assay. Chromatin immunoprecipitation (ChIP) was performed according to a protocol published by Upstate Biotechnologies. AHP-derived oligodendrocytes and the cells cultured with LIF for 2 days were exposed to formaldehyde, at a final concentration of 1%, added directly to the tissue culture medium. Co-immunoprecipitated DNA was used as a template for PCR with the following set of primers: Gfex1S (5′-TGACATCCCAGGAGCCAG-3′) and Gfex1AS (5′-CAGTCTCTCTGCTCACTAGCC-3′).

Animals. MBP-Cre Tg mice (21) were provided by M. Miura (University of Tokyo, Japan). CAG-CAT-EGFP Tg mice (22) were a gift from J. Miyazaki (Osaka University, Japan). All experimental procedures and protocols were approved by the Animal Care and Use Committee of Keio University.

Focal Cerebral Ischemia. Mice were anesthetized by nitrous oxide/oxygen/isoflurane (69/30/1%) administered through an inhalation mask during surgery. Details of surgical procedures are provided in *SI Text*.

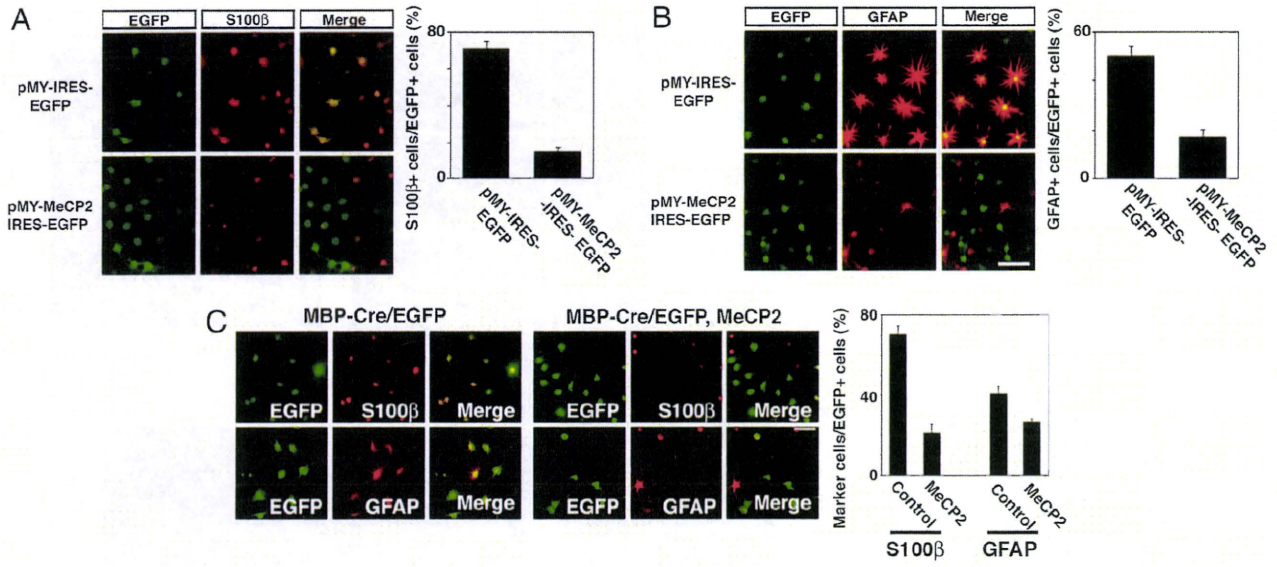

Fig. 5. MeCP2 expression is sufficient for inhibition of astrocyte differentiation of NSCs/NPCs and oligodendrocytes. (*A* and *B*) AHPs were infected with recombinant retrovirus engineered to express only EGFP (pMY), or MeCP2 together with EGFP (pMY-MeCP2-IRES-EGFP), cultured with LIF for 4 days and subjected to immunostaining. GFP (*A* and *B*, green), S100β (*A*, red), GFAP (*B*, red). (Scale bar: 50 μm.) Percentages of S100β- and GFAP-positive cells in EGFP-positive cells were quantified (*Upper* and *Lower* graphs, respectively). Data are mean ± SD. (*C*) AHPs were transfected with MBP-Cre together with CAG-CAT-EGFP and CAG floxed neo, or with CAG-CAT-EGFP and CAG floxed neo-MeCP2, and were allowed to differentiate into oligodendrocytes for 4 days. The cells were then cultured with LIF for an additional 4 days, followed by immunocytochemical staining using antibodies against GFAP and S100β. (Scale bar: 50 μm.) Percentages of GFAP- and S100β-positive cells in EGFP-expressing cells were quantified (*Right*). Data are mean ± SD.

ACKNOWLEDGMENTS. We thank Dr. M. Miura (University of Tokyo) for MBP-Cre transgenic mice, Dr. J. Miyazaki (Osaka University) for CAG-CAT-EGFP transgenic mice, Dr. T. Kitamura (University of Tokyo) for pMY vector and Plat-E cells, Dr. I. Saito (University of Tokyo) for pCALNL5 vector. We appreciate Drs. Y. Bessho and T. Matsui for valuable discussions. We also thank Drs. A. R. Muotri and I. Smith for helpful comments and critical reading of the manuscript. We are very grateful to N. Ueda for excellent secretarial assistance. Many thanks to N. Namihira, Y. Kuromi and K. Tsujimura for technical help. pCALNL5 was provided by RIKEN Brain Research Center, which is participating in the National Bio-Research Project of the Ministry of Education, Culture, Sports, Science and Technology, Japan. This work has been supported by a Grant-in-Aid for Young Scientists; a Grant-in-Aid for Science Research on Priority Areas; the Nara Institute of Science and Technology Global Centers of Excellence Program (Frontier Biosciences: Strategies for Survival and Adaptation in a Changing Global Environment) from the Ministry of Education, Culture, Sports, Science and Technology of Japan; and the Uehara Memorial Foundation.

1. Temple S (2001) The development of neural stem cells. *Nature* 414:112–117.
2. Gage FH (2000) Mammalian neural stem cells. *Science* 287:1433–1438.
3. Hsieh J, Gage FH (2004) Epigenetic control of neural stem cell fate. *Curr Opin Genet Dev* 14:461–469.
4. Bonni A, *et al.* (1997) Regulation of gliogenesis in the central nervous system by the JAK-STAT signaling pathway. *Science* 278:477–483.
5. Nakashima K, *et al.* (1999) Synergistic signaling in fetal brain by STAT3-Smad1 complex bridged by p300. *Science* 284:479–482.
6. Bugga L, Gadient RA, Kwan K, Stewart CL, Patterson PH (1998) Analysis of neuronal and glial phenotypes in brains of mice deficient in leukemia inhibitory factor. *J Neurobiol* 36:509–524.
7. Koblar SA, *et al.* (1998) Neural precursor differentiation into astrocytes requires signaling through the leukemia inhibitory factor receptor. *Proc Natl Acad Sci USA* 95:3178–3181.
8. Nakashima K, *et al.* (1999) Developmental requirement of gp130 signaling in neuronal survival and astrocyte differentiation. *J Neurosci* 19:5429–5434.
9. He F, *et al.* (2005) A positive autoregulatory loop of Jak-STAT signaling controls the onset of astrogliogenesis. *Nat Neurosci* 8:616–625.
10. Jones PA, Baylin SB (2002) The fundamental role of epigenetic events in cancer. *Nat Rev Genet* 3:415–428.
11. Robertson KD, Wolffe AP (2000) DNA methylation in health and disease. *Nat Rev Genet* 1:11–19.
12. Watt F, Molloy PL (1988) Cytosine methylation prevents binding to DNA of a HeLa cell transcription factor required for optimal expression of the adenovirus major late promoter. *Genes Dev* 2:1136–1143.
13. Hendrich B, Bird A (1998) Identification and characterization of a family of mammalian methyl-CpG binding proteins. *Mol Cell Biol* 18:6538–6547.
14. Takizawa T, *et al.* (2001) DNA methylation is a critical cell-intrinsic determinant of astrocyte differentiation in the fetal brain. *Dev Cell* 1:749–758.
15. Fan G, *et al.* (2005) DNA methylation controls the timing of astrogliogenesis through regulation of JAK-STAT signaling. *Development* 132:3345–3356.
16. Suzuki S, *et al.* (2001) Phosphorylation of signal transducer and activator of transcription-3 (Stat3) after focal cerebral ischemia in rats. *Exp Neurol* 170:63–71.
17. Hsieh J, *et al.* (2004) IGF-I instructs multipotent adult neural progenitor cells to become oligodendrocytes. *J Cell Biol* 164:111–122.
18. Shi Y, *et al.* (2004) Expression and function of orphan nuclear receptor TLX in adult neural stem cells. *Nature* 427:78–83.
19. Jenuwein T, Allis CD (2001) Translating the histone code. *Science* 293:1074–1080.
20. Bernstein BE, *et al.* (2006) A bivalent chromatin structure marks key developmental genes in embryonic stem cells. *Cell* 125:315–326.
21. Hisahara S, *et al.* (2000) Targeted expression of baculovirus p35 caspase inhibitor in oligodendrocytes protects mice against autoimmune-mediated demyelination. *EMBO J* 19:341–348.
22. Kawamoto S, *et al.* (2000) A novel reporter mouse strain that expresses enhanced green fluorescent protein upon Cre-mediated recombination. *FEBS Lett* 470:263–268.
23. Levine JM, Reynolds R, Fawcett JW (2001) The oligodendrocyte precursor cell in health and disease. *Trends Neurosci* 24:39–47.
24. Sofroniew MV (2005) Reactive astrocytes in neural repair and protection. *Neuroscientist* 11:400–407.
25. Setoguchi H, *et al.* (2006) Methyl-CpG binding proteins are involved in restricting differentiation plasticity in neurons. *J Neurosci Res* 84:969–979.
26. Jung BP, Zhang G, Ho W, Francis J, Eubanks JH (2002) Transient forebrain ischemia alters the mRNA expression of methyl DNA-binding factors in the adult rat hippocampus. *Neuroscience* 115:515–524.
27. Jessberger S, Toni N, Clemenson GD, Jr, Ray J, Gage FH (2008) Directed differentiation of hippocampal stem/progenitor cells in the adult brain. *Nat Neurosci* 11:888–893.
28. Ballas N, Mandel G (2005) The many faces of REST oversee epigenetic programming of neuronal genes. *Curr Opin Neurobiol* 15:500–506.
29. Colantuoni C, *et al.* (2001) Gene expression profiling in postmortem Rett Syndrome brain: Differential gene expression and patient classification. *Neurobiol Dis* 8:847–865.
30. Lyons SA, Kettenmann H (1998) Oligodendrocytes and microglia are selectively vulnerable to combined hypoxia and hypoglycemia injury in vitro. *J Cereb Blood Flow Metab* 18:521–530.
31. Okada S, *et al.* (2006) Conditional ablation of Stat3 or Socs3 discloses a dual role for reactive astrocytes after spinal cord injury. *Nat Med* 12:829–834.
32. Gage FH, *et al.* (1995) Survival and differentiation of adult neuronal progenitor cells transplanted to the adult brain. *Proc Natl Acad Sci USA* 92:11879–11883.
33. Morita S, Kojima T, Kitamura T (2000) Plat-E: An efficient and stable system for transient packaging of retroviruses. *Gene Ther* 7:1063–1066.
34. Clark SJ, Harrison J, Paul CL, Frommer M (1994) High sensitivity mapping of methylated cytosines. *Nucleic Acids Res* 22:2990–2997.

Neuroscience 155 (2008) 780–788

IDENTIFICATION OF GENES THAT RESTRICT ASTROCYTE DIFFERENTIATION OF MIDGESTATIONAL NEURAL PRECURSOR CELLS

T. SANOSAKA,[a] M. NAMIHIRA,[a] H. ASANO,[a] J. KOHYAMA,[a] K. ISAKI,[b] K. GARASHI,[b] J. KANNO[b] AND K. NAKASHIMA[a]*

[a]*Laboratory of Molecular Neuroscience, Graduate School of Biological Sciences, Nara Institute of Science and Technology, 8916-5, Takayama, Ikoma, Nara 630-0101, Japan*

[b]*Division of Cellular and Molecular Toxicology, Biological Safety Research Center, National Institutes of Health Sciences, 1-18-1, Kamiyoga, Setagaya-ku, Tokyo 158-8501, Japan*

Abstract—During development of the mammalian CNS, neurons and glial cells (astrocytes and oligodendrocytes) are generated from common neural precursor cells (NPCs). However, neurogenesis precedes gliogenesis, which normally commences at later stages of fetal telencephalic development. Astrocyte differentiation of mouse NPCs at embryonic day (E) 14.5 (relatively late gestation) is induced by activation of the transcription factor signal transducer and activator of transcription (STAT) 3, whereas at E11.5 (mid-gestation) NPCs do not differentiate into astrocytes even when stimulated by STAT3-activating cytokines such as leukemia inhibitory factor (LIF). This can be explained in part by the fact that astrocyte-specific gene promoters are highly methylated in NPCs at E11.5, but other mechanisms are also likely to play a role. We therefore sought to identify genes involved in the inhibition of astrocyte differentiation of NPCs at midgestation. We first examined gene expression profiles in E11.5 and E14.5 NPCs, using Affymetrix GeneChip analysis, applying the Percellome method to normalize gene expression level. We then conducted *in situ* hybridization analysis for selected genes found to be highly expressed in NPCs at midgestation. Among these genes, we found that *N-myc* and high mobility group AT-hook 2 (*Hmga2*) were highly expressed in the E11.5 but not the E14.5 ventricular zone of mouse brain, where NPCs reside. Transduction of *N-myc* and *Hmga2* by retroviruses into E14.5 NPCs, which normally differentiate into astrocytes in response to LIF, resulted in suppression of astrocyte differentiation. However, sustained expression of *N-myc* and *Hmga2* in E11.5 NPCs failed to maintain the hypermethylated status of an astrocyte-specific gene promoter. Taken together, our data suggest that astrocyte differentiation of NPCs is regulated not only by DNA methylation but also by genes whose expression is controlled spatio-temporally during brain development. © 2008 IBRO. Published by Elsevier Ltd. All rights reserved.

Key words: *N-myc*, *Hmga2*, epigenetics, Percellome method, differentiation.

The mammalian CNS is composed of neurons, astrocytes, and oligodendrocytes. Although these three cell types are derived from common multipotent neural precursor cells (NPCs), their differentiation is spatially and temporally regulated during development (Temple, 2001). Fetal telencephalic NPCs divide symmetrically in early gestation to increase their own numbers, and then undergo neurogenesis through mostly asymmetric divisions. Toward the end of the neurogenic phase, NPCs acquire multipotentiality to generate astrocytes and oligodendrocytes as well as neurons. It has recently become apparent that NPC fate determination is controlled by both extracellular cues, including cytokine signaling, and intracellular programs such as epigenetic gene regulation (Edlund and Jessell, 1999; Takizawa et al., 2001; Hsieh and Gage, 2004).

Interleukin (IL) -6 family cytokines such as cardiotrophin-1 (CT-1), leukemia inhibitory factor (LIF) and ciliary neurotrophic factor (CNTF) activate the janus kinase (JAK) –signal transducer and activator of transcription (STAT) signaling pathway and are known to induce astrocyte differentiation of NPCs (Bonni et al., 1997; Rajan and McKay, 1998). Gene knockouts of LIF (Bugga et al., 1998), LIF receptor β (Koblar et al., 1998), the common receptor component gp130 (Nakashima et al., 1999a) and STAT3 (He et al., 2005) all result in impaired astrocyte differentiation *in vivo*, emphasizing the contribution of JAK-STAT signaling to astrogliogenesis in the developing CNS. Bone morphogenetic proteins (BMPs) are another group of astrocyte-inducing cytokines. They synergistically induce astrocytic differentiation of NPCs via formation of a complex between STATs and BMP-activated transcription factor Smads, bridged by the transcriptional coactivators p300/CBP (Nakashima et al., 1999b).

In addition to these extracellular factors, intracellular programs and factors also play critical roles to regulate astrocytic differentiation of NPCs. We have previously shown that a CpG dinucleotide within a STAT3-binding element (TTCCGAGAA) in the astrocytic marker glial fibrillary acidic protein (*gfap*) gene promoter is highly methylated in NPCs at midgestation (embryonic day (E)11.5), when the cells differentiate only into neurons but not into astrocytes. Since STAT3 does not bind to the methylated cognate sequence, NPCs at midgestation do not express *gfap* even when stimulated by STAT3-activating cytokines such as LIF. As gestation proceeds, the STAT3-binding

*Corresponding author. Tel: +81-743-72-5471; fax: +81-743-72-5479.
E-mail address: kin@bs.naist.jp (K. Nakashima).

Abbreviations: bHLH, basic helix–loop–helix; BMP, bone morphogenetic protein; CNTF, ciliary neurotrophic factor; CT-1, cardiotrophin-1; DIG, digoxigenin; E, embryonic day; Gapdh, glyceraldehyde-3-phosphate dehydrogenase; GEO, Gene Expression Omnibus; *gfap*, glial fibrillary acidic protein; *Hmga2*, high mobility group AT-hook 2; JAK, janus kinase; LIF, leukemia inhibitory factor; NPC, neural precursor cell; SSC, sodium chloride sodium citrate; STAT, signal transducer and activator of transcription.

0306-4522/08$32.00+0.00
doi:10.1016/j.neuroscience.2008.06.039

site becomes gradually demethylated in NPCs, enabling them to express *gfap* in response to LIF stimulation (Takizawa et al., 2001). Thus, we have proposed that DNA methylation is a critical cell-intrinsic determinant of astrocyte differentiation during brain development. However, the important question of how this astrocyte-specific gene promoter becomes demethylated in NPCs remains unanswered.

Neurogenic basic helix–loop–helix (bHLH) transcription factors have been also shown to regulate astrocyte differentiation during early neural development. Mice carrying mutations in *mash1* and *math3* (Tomita et al., 2000), or, to a lesser extent, *mash1* and *ngn2* (Nieto et al., 2001) exhibit decreased neurogenesis and premature astrogliogenesis. Conversely, overexpression of neurogenic bHLH factors, either *in vivo* during the gliogenic period (Cai et al., 2000) or in cultured NPCs exposed to CNTF (Sun et al., 2001), promotes neurogenesis at the expense of astrogliogenesis. A possible mechanism underlying the repressive effect on astrogliogenesis is that Ngn1 binds to p300/CBP and sequesters them away from STAT3, thereby preventing STAT3 from activating astrocytic gene expression (Sun et al., 2001). Such a mechanism may ensure the restriction of astrocyte differentiation in NPCs that would otherwise differentiate into neurons under the influence of high-level neurogenic bHLH factor expression during the neurogenic period.

Although these studies have provided us with an integrated insight into the mechanism of neurogenic-to-gliogenic switching in NPCs, they do not preclude the involvement of other, as yet unknown, factors. To identify such factors, we first in this study examined gene expression profiles of mid- and late-gestational NPCs by Affymetrix GeneChip analysis, which is widely used to obtain a complete picture of developmental stage-specific gene expression (Abramova et al., 2005; Ajioka et al., 2006). We then performed *in situ* hybridization experiments to investigate the spatio-temporal expression pattern of genes that were found to be highly expressed in midgestational NPCs. Two genes, *N-myc* and high mobility group AT-hook 2 (*Hmga2*), were highly expressed in the ventricular zone of E11.5 but not of E14.5 mouse brain. Transduction of *N-myc* and *Hmga2* into E14.5 NPCs resulted in suppression of astrocyte differentiation, even in the presence of LIF. However, the prolonged expression of these genes in E11.5 NPCs failed to preserve the hypermethylated status of the astrocyte-specific *gfap* promoter. These results suggest that the inhibition of astrocyte differentiation in midgestational NPCs is regulated not only by DNA methylation of astrocyte-specific gene promoters but also by transcription-regulating factors whose expression is controlled spatio-temporally during brain development.

EXPERIMENTAL PROCEDURES

NPC culture

Timed-pregnant ICR mice were used to prepare NPCs. The protocols described below were carried out according to the animal experimentation guidelines of Nara Institute of Science and Technology that comply with National Institutes of Health Guide for Care and Use of Laboratory Animals. All efforts were made to minimize the number of animals used and their suffering. NPCs were prepared from telencephalons of E11.5 and E14.5 mice and cultured as described previously (Nakashima et al., 1999b). Briefly, the telencephalons were triturated in Hanks' balanced salt solution by mild pipetting with a 1-ml pipet tip (Gilson, Middleton, WI, USA). Dissociated cells were cultured in N2-supplemented Dulbecco's Modified Eagle's Medium with F12 (GIBCO, Grand Island, NY, USA) containing 10 ng/ml basic FGF (R&D Systems, Minneapolis, MN, USA) (N2/DMEM/F12/bFGF) on culture dishes (Nunc, Naperville, IL, USA) or chamber slides (Nunc) which had been precoated with poly-L-ornithine (Sigma, St. Louis, MO, USA) and fibronectin (Sigma).

Immunocytochemistry

E11.5 and E14.5 NPCs cultured on coated chamber slides were washed with PBS, fixed in 4% paraformaldehyde in PBS, and stained with the following primary antibodies: rabbit anti-SOX2 (1:1000, Chemicon, Temecula, CA, USA), mouse anti-βIII-tubulin (1:500, Sigma), rabbit anti-GFAP (1:2000, Dako, High Wycombe, UK). The following secondary antibodies were used: Alexa488-conjugated goat anti-rabbit IgG (1:500, Molecular Probes, Eugene, OR, USA), Cy3-conjugated goat anti-mouse IgG (1:500, Chemicon). Nuclei were stained using bisbenzimide H33258 fluorochrome trihydrochloride (Nacalai Tesque, Kyoto, Japan). All experiments were independently replicated at least three times.

Sample preparation and GeneChip analysis

These procedures were conducted according to the Percellome method (Kanno et al., 2006) to normalize mRNA expression values to sample cell numbers by adding external spike mRNAs to the sample in proportion to the genomic DNA concentration and utilizing the spike RNA quantity data as a dose-response standard curve for each sample. Cells cultured on coated dishes were washed with PBS, lysed in 500 ml of RLT buffer (Qiagen K.K., Tokyo, Japan) and transferred to a 1.5-ml tube. Two separate 10-μl aliquots were treated with DNAse-free RNase A (Nippon Gene, Tokyo, Japan) for 30 min at 37 °C, followed by proteinase K (Roche Diagnostics, Mannheim, Germany) for 3 h at 55 °C, and then transferred to a 96-well black plate. PicoGreen fluorescent dye (Molecular Probes) was added to each well, and then incubated for 2 min at 30 °C. The DNA concentration was measured using a 96-well fluorescence plate reader with excitation at 485 nm and emission at 538 nm. Lamda phage DNA (PicoGreen kit, Molecular Probes) was used as standard. The appropriate amount of spike RNA cocktail was added to the sample homogenates in proportion to their DNA concentration. Five independent *Bacillus subtilis* poly-A RNAs were included in the grade-dosed spike cocktail. Total RNAs were purified using an RNeasy Mini kit (Qiagen), according to the manufacturer's instructions. First-strand cDNAs were synthesized by incubating 5 μg of total RNA with 200 U SuperScript II reverse transcriptase (Invitrogen, Carlsbad, CA, USA) and 100 pmol T7-$(dT)_{24}$ primer [5′-GGCCAGTGAATTGTAATACGACTCACTATAGGGAGGCGG-$(dT)_{24}$-3′]. After second-strand synthesis, the double-stranded cDNAs were purified using a GeneChip Sample Cleanup Module (Affymetrix, Washington, DC, USA), according to the manufacturer's instructions, and labeled by *in vitro* transcription using a BioArray HighYield RNA transcript labeling kit (Enzo Life Sciences, Farmingdale, NY, USA). The labeled cRNA was then purified using a GeneChip Sample Cleanup Module (Affymetrix) and treated with fragmentation buffer at 94 °C for 35 min. For hybridization to a GeneChip Mouse Genome 430 2.0 Array (Affymetrix), 15 μg of fragmented cRNA probe was incubated with 50 pM control oligonucleotide B2, 1× eukaryotic hybridization control (1.5 pM BioB, 5 pM BioC, 25 pM BioD and 100 pM Cre), 0.1 mg/ml herring sperm

DNA, 0.5 mg/ml acetylated BSA and 1× manufacturer-recommended hybridization buffer in a 45 °C rotisserie oven for 16 h. Washing and staining were performed in a GeneChip Fluidics Station (Affymetrix) using the appropriate antibody amplification, washing and staining protocols. The phycoerythrin-stained arrays were scanned as digital image files, which were analyzed with GeneChip Operating Software (Affymetrix). The expression data were converted to copy numbers of mRNA per cell by the Percellome method, quality controlled, and analyzed using Percellome software (Kanno et al., 2006). The GeneChip data have been deposited in the NCBI Gene Expression Omnibus (GEO; http://www.ncbi.nlm.nih.gov/geo/) and is accessible through GEO series accession number GSE 10796.

Quantitative real-time RT-PCR

Quantitative real-time PCR was performed to confirm the results of GeneChip analysis. RNAs from E11.5 and E14.5 NPCs were reverse transcribed using Superscript II (Invitrogen) and amplified by PCR, with a specific pair of primers for each gene, using the Mx3000P system (Stratagene, La Jolla, CA, USA). The expression of target genes was normalized to that of glyceraldehyde-3-phosphate dehydrogenase (*Gapdh*). The gene-specific primers were as follows: mouse N-myc: N-myc-S, 5′-aactatgctgcaccctcacc-3′; N-myc-AS, 5′-tagcaagtccgagcgtgttc-3′; mouse Hmga2: Hmga2-S, 5′-ggcagccgtccacatcag-3′; Hmga2-AS, 5′-taatcctcctctgcggactc-3′; mouse Sox11: Sox11-S, 5′-gagcctgtacgacgaagtgc-3′; Sox11-AS, 5′-tgaacaccaggtcggagaag-3′; mouse Bhlhb5: Bhlhb5-S, 5′-gttgcgcctcaacatcaac-3′; Bhlhb5-AS, 5′-acttttgcagaggctggac-3′; mouse Bcl11a: Bcl11a-S, 5′-gcatcaagctggagaaggag-3′; Bcl11a-AS, 5′-gagcttccatccgaaaactg-3′; mouse Gapdh: Gapdh-S, 5′-accacagtccatgccatcac-3′; Gapdh-AS, 5′-tccaccaccctgttgctgta-3′.

In situ hybridization

Digoxigenin- (DIG; Roche) labeled cRNA probes were synthesized for each gene, following the manufacturer's instructions. Cryosections were washed with PBS and fixed with 4% PFA. After fixation, sections were incubated in prehybridization solution (5× sodium chloride sodium citrate (SSC), 1% SDS, 50 μg/ml yeast transfer RNA, 50 μg/ml heparin in 50% formamide) at 70 °C for 1 h and hybridized with 500 ng/ml of DIG-labeled cRNA probes at 65 °C for 16 h. After three washes with wash solution 1 (5× SSC, 1% SDS in 50% formamide) and wash solution 3 (2× SSC in 50% formamide), sections were blocked with 10% normal sheep serum in TBST at room temperature for 1 h and then incubated with 1:1000 alkaline phosphatase-conjugated anti-DIG antibody (Roche) at 4 °C for 16 h. After four washes with TBST, hybridized probes were visualized with 5-bromo-4-chloro-3 indolylphosphate and nitro blue tetrazolium chloride.

Recombinant retrovirus construction and infection

Human *N-myc* and mouse *Hmga2* cDNAs were cloned into the expression vector pMYs, which contains an internal ribosome entry site followed by the region upstream of the *EGFP* gene (Morita et al., 2000). The Plat-E packaging cell line was transiently transfected with the retrovirus DNA by Trans-IT 293 (Mirus, Madison, WI, USA) (Morita et al., 2000). On the following day, the medium was replaced with N2/DMEM/F12/bFGF, and the cells were cultured in this medium for 1 day before virus was collected.

Fluorescence activated cell sorting

Virus-infected E11.5 NPCs were cultured for 4 days, after which GFP-labeled cells were sorted using a FACS Vantage (Becton Dickinson, Franklin Lakes, NJ, USA) at a flow rate of less than 1500 events/s; gating parameters were set by side and forward scatter to eliminate debris, dead and aggregated cells. After sorting, genomic DNA was extracted and used for bisulfite sequencing.

Bisulfite sequencing

Sodium bisulfite treatment of genomic DNA was performed using a Methylamp DNA Modification kit (Epigentek, Brooklyn, NY, USA), according to the manufacturer's instructions. The region in the *gfap* promoter containing the STAT-binding site of the bisulfite-treated genomic DNA was amplified by PCR using the following primers: GFmS (5′-GGGATTTATTAGGAGAATTTTAGAAGTAG-3′), GFmAS (5′-TCTACCCATACTTAAACTTCTAATATCTAC-3′). The PCR products were cloned into pT7Blue vector (Novagen, Madison, WI, USA) and at least 12 randomly selected clones were sequenced.

RESULTS

Preparation of NPCs from different developmental stages and comparison of their gene expression profiles by GeneChip analysis

E11.5 NPCs do not differentiate into astrocytes, even in the presence of the astrocyte-inducing cytokine LIF, in contrast to 4-day cultured E14.5 NPCs (Takizawa et al., 2001). As a first step toward identifying factors involved in the inhibition of astrocyte differentiation of NPCs at midgestation, we examined the gene expression profiles of E11.5 and E14.5 NPCs.

E11.5 and E14.5 NPCs were isolated from embryonic telencephalon and cultured as indicated in Fig. 1A. To evaluate the purity of NPCs in each cell population, the cells were stained with antibody against SOX2, an NPC marker (Graham et al., 2003). As shown in Fig. 1B and C, the majority of cells in both populations were positive for SOX2, indicating that NPCs were highly enriched. An Affymetrix mouse genome GeneChip array was chosen to compare expression profiles in the two populations, and we adopted the Percellome method to normalize gene expression from different samples (Kanno et al., 2006). The method enabled us to quantify mRNA molecules per cell based on the measurement of cell by adding a grade-dosed spike cocktail to the samples. We excluded genes whose transcript copy number was below six per cell. Scatter plots illustrating the differences between E11.5 and E14.5 NPCs are shown in Fig. 1D; 194 genes were expressed at >fivefold higher level in E11.5 NPCs than in E14.5 NPCs (Fig. 1D, light blue zone). Of these, 102 were known genes, and were classified by functional category (Fig. 1E). Since we wished to identify negative regulators of astrocyte differentiation, or factors involved in the epigenetic modification in midgestational NPCs, we focused on transcription-related genes (Fig. 1E, red). These 21 genes are listed in Table 1, and five (*N-myc*, *Hmga2*, *Bhlhb5*, *Sox11*, *Bcl11a*) were selected for further analysis because they have been reported to play roles in cell growth, differentiation, and chromatin remodeling in other types of stem cells (Sawai et al., 1990; Zhou et al., 1995; Saiki et al., 2000; Knoepfler et al., 2002; Brunelli et al., 2003; Sock et al., 2004).

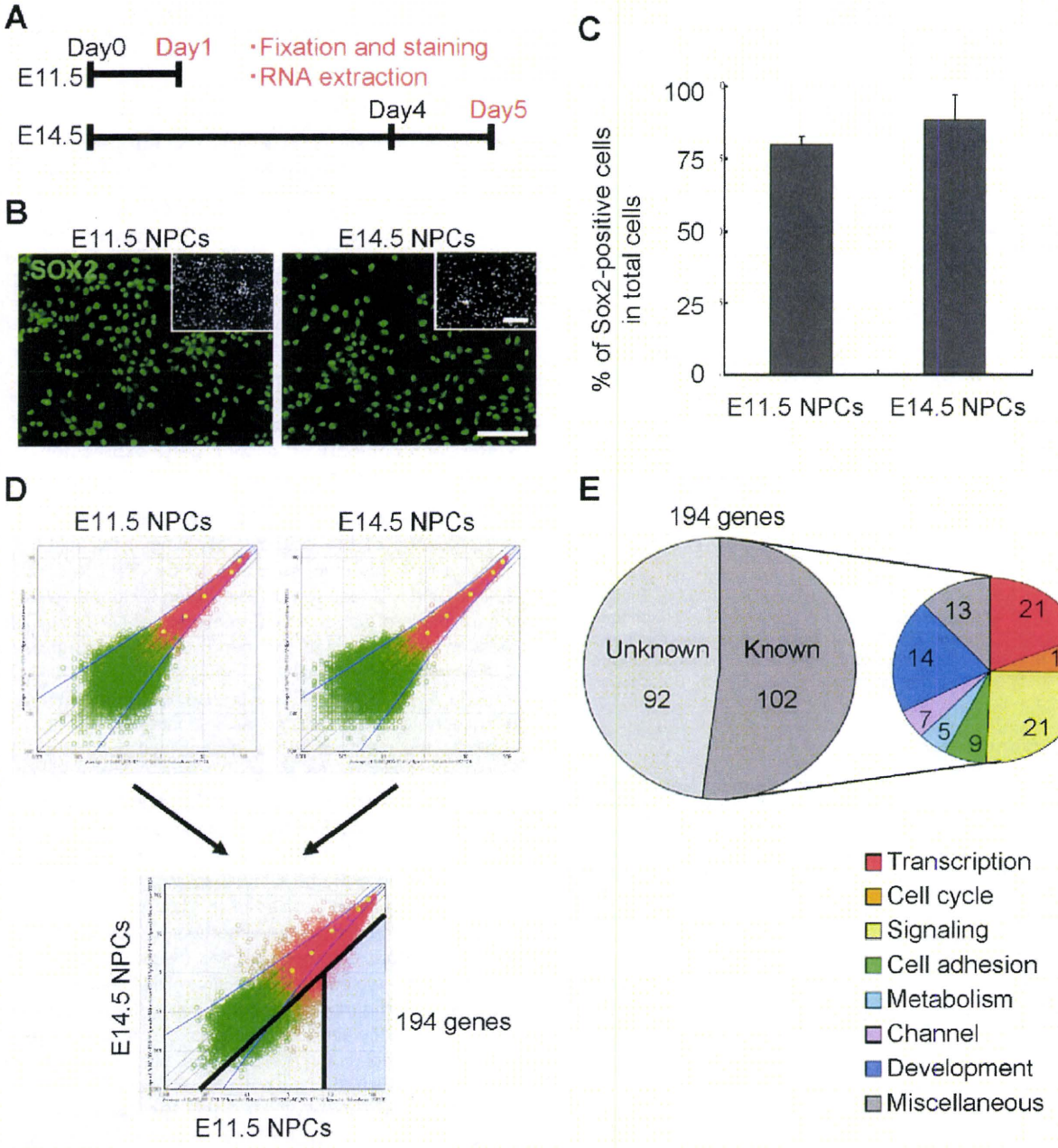

Fig. 1. Comparison of gene expression profiles in E11.5 and E14.5 NPCs. (A) Schematic of experimental protocol. NPCs isolated from E11.5 mouse telencephalon were plated (day 0) and used on the following day for immunostaining and RNA extraction (day 1). NPCs isolated at E14.5 were expanded for 4 days and replated on day 4. On day 5, these cells were fixed for immunostaining. RNA was also extracted. (B) E11.5 and E14.5 NPCs were stained with antibody against Sox2 (green). Scale bar=25 μm. Insets: Hoechst nuclear staining of each field. Scale bar=25 μm. (C) The percentage of Sox2-positive cells in E11.5 and E14.5 NPCs was quantified. Mean±S.D. (D) Scatter plots of E11.5 (upper left) and E14.5 (upper right) samples obtained from GeneChip analysis indicated no significant change between independent experiments with the same sample. Overview (lower plot) of gene expression change was compared between each sample. One hundred ninety-four genes were expressed at >fivefold higher level in E11.5 NPCs than E14.5 NPCs (light blue zone). (E) Of the 194 genes that were highly expressed in E11.5 NPCs, known genes were classified according to Affymetrix gene ontology. For interpretation of the references to color in this figure legend, the reader is referred to the Web version of this article.